

Decreased expression of the candidate tumor suppressor gene *ING1* is associated with poor prognosis in advanced neuroblastomas

MASATO TAKAHASHI^{1,2}, TOSHINORI OZAKI¹, SATORU TODO² and AKIRA NAKAGAWARA¹

¹Division of Biochemistry, Chiba Cancer Center Research Institute, 666-2 Nitona, Chuoh-ku, Chiba 260-8717;

²First Department of Surgery, Hokkaido University School of Medicine, N15 W7, Kita-ku, Sapporo 060-8638, Japan

Received January 27, 2004; Accepted March 30, 2004

Abstract. *ING1* has been identified as a novel candidate tumor suppressor gene using a genetic suppressor element (GSE) strategy. Ectopic expression of *ING1* in mammalian cultured cells causes cell cycle arrest and apoptosis through a p53-dependent and/or p53-independent pathway. However, there has been no report on the prognostic significance of the *ING1* expression level in human cancers, though the expression of the wild-type *ING1* gene is significantly decreased in breast, lymphoid and gastric cancers as compared with their corresponding normal tissues. In order to explore the possible involvement of *ING1* in tumorigenesis of neuroblastoma, we examined the expression levels of *ING1* mRNA in 32 primary neuroblastomas by using a quantitative real-time PCR. *ING1* mRNA was expressed independently of the disease stages. However, low levels of *ING1* mRNA were significantly associated with a poor prognosis (log-rank test, $p=0.017$). Multivariate analysis showed that the expression level of *ING1* was closely related to survival ($p=0.020$), even after controlling with age ($p=0.008$) or stage ($p=0.025$), while it was only marginally significant after controlling with *TrkA* expression ($p=0.063$). Mutation analysis revealed that there was no mutation or deletion of the *ING1* gene except 1 silent mutation at codon 188 in primary neuroblastomas examined. Taken together, our results suggest for the first time that a decreased level of *ING1* expression is a novel indicator of poor prognosis in advanced stages of neuroblastoma, and that *ING1* may play a crucial role in genesis and progression of neuroblastoma.

Introduction

Neuroblastoma, which is derived from the sympathoadrenal lineage of the neural crest, is one of the most common pediatric

solid tumors (1). Neuroblastoma is an enigmatic tumor and shows distinct biology in 2 subsets. A subset of tumors in early stages has favorable prognosis and usually occurs in patients <1 year of age. They have no amplification of the *MYCN* oncogene and often differentiate and/or regress spontaneously. In contrast, the other is a subset of tumors in the advanced stages with poor prognosis, which usually possesses *MYCN* amplification and allelic loss in the distal region of the short arm of chromosome 1. However, there is an intermediate type of neuroblastoma which displays advanced phenotypes but has no *MYCN* amplification (2). From the clinical point of view, the latter type of neuroblastoma is the most problematic, and it is quite difficult to decide which therapeutic strategy should be chosen.

ING1 has been identified as a novel candidate tumor suppressor gene by using a novel strategy, which combines a subtractive hybridization and *in vivo* selection system (genetic suppressor elements method, GSE) (3,4). The *ING1* gene encodes a nuclear protein with a molecular mass of 33 kDa, which exhibits no significant homology with known proteins filed in the public databases. According to the recent reports, there exist at least 3 *ING1* variants arising from alternative splicing of mRNA (5,6). It has been mapped to human chromosome 13q33-q34, the region of which is known to be involved in the progression of various cancers (7-10). Expression of *ING1* is regulated in a cell cycle-dependent manner, reaching a maximal level during the S-phase (11-13). Ectopic expression of *ING1* in certain mammalian cultured cells results in a cell cycle arrest at the G0/G1 phase, suggesting that *ING1* acts as a potent growth regulator (4). Furthermore, the physical and functional interaction of *ING1* with tumor suppressor p53 has been reported and this could be one of the key mechanisms of the p53-mediated growth regulation (14). In addition, mutation of *ING1* which generates a truncated protein has been found in one of the neuroblastoma cell lines (4), suggesting that *ING1* might be involved in genesis and/or progression of neuroblastoma.

To confirm this possibility, we performed mutation analysis of the *ING1* gene and also examined the expression levels of *ING1* mRNA in 32 primary neuroblastoma tissues. Although we did not detect any mutations or deletions, we found a significant decrease in the expression levels of *ING1* mRNA

Correspondence to: Dr Akira Nakagawara, Division of Biochemistry, Chiba Cancer Center Research Institute, 666-2 Nitona, Chuoh-ku, Chiba 260-8717, Japan
E-mail: akiranak@chiba-ccri.chuo.chiba.jp

Key words: *ING1*, neuroblastoma, p53, prognostic factor

in neuroblastoma tissues derived from patients who died of the disease. Thus, our present study suggests that the decreased level of *ING1* expression is a novel indicator of poor prognosis in advanced neuroblastoma.

Materials and methods

Patients and tumor tissues. Among 32 samples, 11 cases were identified by a mass screening program for neuroblastoma that began in 1985 in Japan. Eight tumors were obtained from patients treated at the Pediatric Oncology Group Institutions or other institutions in the United States. All tumors were diagnosed by histologic assessment. These consisted of 4 ganglioneuroblastomas and 28 neuroblastomas, all of which were considered neuroblastomas in these analyses. Staging was performed according to the staging system described by Evans *et al.* (15), and identified 9 stage I, 4 stage II, 7 stage III, 5 stage IV and 7 stage IVs. All of the patients were treated according to previously described protocols (16-20). Despite differences between the protocols for the Japanese patients and those for the patients treated by the Pediatric Oncology Group, drugs and their doses were similar and the stage-specific survival rates obtained by these 2 groups did not differ significantly (data not shown). The median follow-up period after diagnosis was 26 months (range, 7-63). None of the patients underwent bone marrow transplantation.

Southern hybridization. The *MYCN* gene amplification was examined by Southern analysis. High molecular weight genomic DNA prepared from frozen neuroblastoma tissues was digested completely with *EcoRI*, separated by 1% agarose gel electrophoresis and transferred onto a nylon membrane filter. The filter was fixed by UV irradiation and hybridized at 42°C in a solution containing 6X SSC, 5X Denhardt's solution, 0.5% SDS and ³²P-labeled *MYCN* DNA. After hybridization, the filter was washed extensively at 50°C in 0.1X SSC containing 0.1% sarcosine and exposed to X-ray film with an intensifying screen at -70°C. The *MYCN* copy number was determined as described previously (21).

Northern blot analysis. Total RNA was extracted from 0.5-1.0 g of frozen neuroblastoma tissues using a standard guanidine thiocyanate extraction procedure (22). Total RNA (20 µg) was electrophoresed in 1% agarose gel under denaturing conditions and transferred by capillary onto nylon membrane filters. Hybridization was conducted at 42°C under the standard conditions in 6X SSC, 5X Denhardt's solution, 0.5% SDS and a radio-labeled cDNA probe for *TrkA* and *p53*. After hybridization, filters were washed at room temperature in 2X SSC/0.1% sarcosine followed by 2 washes at 50°C in 0.1X SSC containing 0.1% sarcosine and then exposed to X-ray film with an intensifying screen at -70°C. To normalize the expression level of genes of interest, filters were stripped of probes and rehybridized with a radio-labeled cDNA encoding *β-actin*. The intensity of each specific band was measured by a densitometric scanning, and the expression level of each gene was expressed as arbitrary density units. The distinction between high and low level of *TRK-A* expression was based on the value of the histogram that gave the best natural separation (23).

Quantitative RT-PCR analysis. The expression level of *ING1* was measured by a real-time RT-PCR method (24). Total RNA (2 µg) was converted to first-strand cDNA using Superscript II reverse transcriptase (Life Technologies, Rockville, MD, USA). The PCR amplification was performed with the following primers: *ING1* sense (725F) (5'-AGATGATCGGCTGCGACAA-3') and antisense (1038R) (5'-TCCCTATGAAAGGATGGTTCC-3'). The probe oligonucleotide (952T) (5'-TACATTGCCTTTGTTGAGGTGCAT-3') which hybridizes with the target sequences of the PCR products, was labeled with a reporter fluorescent dye (FAM, 6-carboxy-fluorescein) and a quencher fluorescent dye (TAMRA, 6-carboxytetramethyl-rhodamine) at its 5'- and 3'-end, respectively. PCR was carried out in a 25 µl reaction mixture containing 0.2 µM of each primer, 0.3 mM dATP, 0.3 mM dGTP, 0.3 mM dCTP, 0.6 mM dUTP instead of dTTP, 4 mM Mn(OAc)₂, 1X TaqMan EZ Buffer A, 0.25 units of AmpErase uracil N-glycosylase, 0.625 units of AmpliTaq Gold and 0.1 µM probe oligonucleotide. Reaction mixtures were pre-incubated at 50°C for 2 min, 95°C for 5 min and then subjected to 40 cycles of 95°C for 20 sec and 62°C for 1 min using ABI Prism 7700 Sequence Detector (PE Applied Biosystems). During the PCR amplification, the fluorescent-labeled probe was hydrolyzed by the activity of AmpliTaq Gold and the reporter dye was released from the probe oligonucleotide. The resulting increase in the reporter fluorescent emission was monitored in real-time. The expression level of *ING1* was normalized to that of *β-actin* which was detected by the same real-time RT-PCR method.

RT-PCR SSCP analysis and DNA sequencing. For the detection of *ING1* mutation, we designed 4 primer sets which cover the entire coding region of human *ING1*. The reaction mixture contained 1 µl of the cDNA synthesized, 1 µM of each primer, 200 nM dNTPs, 1X reaction buffer, 0.15 units DNA polymerase (Expand High Fidelity PCR system) and [α-³²P]dCTP. PCR was performed as follows: pre-heating at 96°C for 3 min followed by 35 cycles of 96°C for 30 sec, 56°C for 30 sec and 72°C for 30 sec with final extension at 72°C for 5 min. PCR products were mixed with 1/10 volume of a loading buffer containing 95% formamide, 20 mM EDTA, 0.05% bromophenol blue and 0.05% xylene cyanol, denatured at 98°C for 5 min, and quenched on ice. Electrophoresis was carried out on 5% polyacrylamide gel with 5% glycerol at room temperature at 200 V for 15 h. After electrophoresis, the gel was dried and exposed to X-ray film with an intensifying screen at -70°C.

To determine nucleotide sequences of PCR products, they were purified by the GenElute Agarose Spin Column (Supelco, Bellefonte, PA, USA), subcloned into pGEM-T Easy Vector (Promega, Madison, WI, USA), and sequenced by the dideoxy chain termination method using the ABI Prism 377 DNA sequencer (Perkin-Elmer, Foster City, CA, USA).

Statistical analysis. A possible association between the *ING1* expression level and all prognostic factors was investigated using the Mann-Whitney U test. Pearson correlation with Bonferroni-adjusted significance levels were calculated between expression levels of all genes examined. Since the values of mRNA expression were skewed, a log or Box-cox

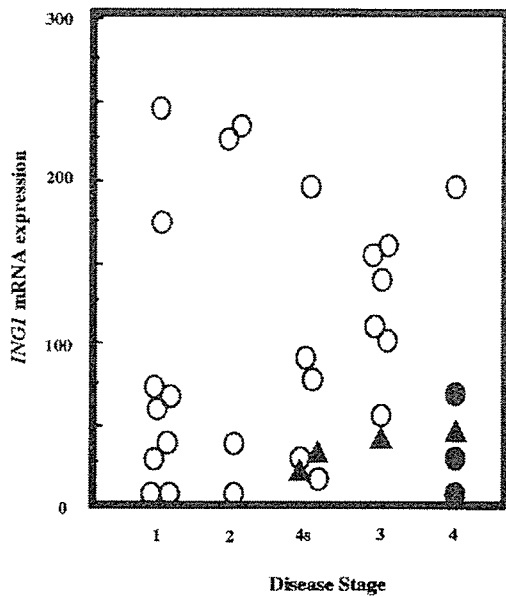


Figure 1. Expression of *ING1* mRNA in primary neuroblastomas. Total RNA was prepared from the indicated primary neuroblastoma tissues, and subjected to a quantitative real-time RT-PCR analysis as described under Materials and methods. The ratios of *ING1* mRNA levels to β -actin mRNA levels were quantified and are indicated as a fold change on the y axis. Nine in stage I, 4 in stage II, 7 in stage III, 5 in stage IV and 7 in stage IVs. (○), alive; (●), dead with single copy of *MYCN*; (▲), dead with *MYCN* amplification.

transformation was used to achieve the normality when calculating correlation coefficients. Comparisons between 2 clinical or biological variables were carried out using the χ^2 analysis. The Kaplan-Meier life table analysis was applied to compare individual variables and survival, and different survival curves were compared using the log-rank test. Cox regression models were used to explore the association between the expression of *ING1* and age, tumor stage, *MYCN*, *TRK-A* or survival. We considered $p > 0.05$ to be significant. Statistical analyses were performed using the StatView version 4.5 (Abacus Concept Inc. Berkeley, CA, USA) and Stata version 6.0. (Stata Corporation, TX, USA).

Results

Mutation analysis of *ING1* gene in human neuroblastoma.

Recently, it has been reported that one of the human neuroblastoma cells, SK-N-SH, carries a mutation of the *ING1* gene, which generates a truncated form of *ING1* (4). To search for mutation of the *ING1* gene in 32 primary neuroblastoma tissues, we performed RT-PCR-single strand conformation polymorphism (SSCP) analysis, followed by subsequent DNA sequencing according to the procedure as described previously (25,26). Among 32 samples examined, the PCR product amplified from 1 case of neuroblastoma in stage I displayed an aberrantly migrating band, however, DNA sequencing analysis revealed that this aberrant band reflected a silent mutation at codon 188 [Ser188Ser (TCG-TCA)] (data not shown).

*Down-regulation of *ING1* mRNA is associated with unfavorable prognosis of neuroblastoma.* We then examined

Table I. The results of log-rank tests for conventional prognostic factors and expression of *ING1* and *p53* in 32 primary neuroblastomas.

Variable	Number of subjects	Number of deaths (%)	Number of expected deaths	p-value
<i>ING1</i> expression				.017
Low	16	6 (37.5)	2.96	
High	16	1 (6.3)	4.04	
<i>p53</i> expression				.250
Not expressed	7	2 (28.6)	0.98	
Expressed	22	3 (13.6)	4.02	
Age				.001
<1 year	19	1 (5.3)	4.93	
>1 year	12	6 (50.0)	2.07	
Origin				.077
Adrenal gland	24	7 (100)	4.89	
Others	8	0 (0)	2.11	
Disease stage				.044
I+II+IVs	20	2 (10.0)	4.53	
III+IV	12	5 (41.7)	2.47	
<i>MYCN</i> copy number				<.0001
Amplified	4	4 (100)	0.39	
Single copy	28	3 (10.7)	6.61	
Trk-A expression				.0032
Low	6	3 (50.0)	0.78	
High	24	2 (8.3)	4.28	

ING1 expression levels in primary neuroblastomas because epigenetic regulation of the tumor suppressor genes are involved in the genesis and/or progression of many human cancers (27). Since the expression levels of *ING1* mRNA were below the detectable levels by Northern blot hybridization, we performed a quantitative real-time RT-PCR (24) to measure its expression levels in 32 neuroblastoma tissues. The threshold cycle number value (C_T), indicating the relative levels of *ING1* mRNA (after normalization to that of β -actin mRNA) was in the range of 0-250 (median value, 64). As shown in Fig. 1, there were no statistically significant differences in expression levels of *ING1* mRNA among the disease stages (mean \pm SEM; stage I, 79 ± 27 , $n=9$; stage II, 126 ± 59 , $n=4$; stage IVs, 67 ± 24 , $n=7$; stage III, 110 ± 17 , $n=7$; stage IV, 70 ± 33 , $n=5$; $p > 0.05$). Note that *ING1* expression levels were significantly decreased in the tumors obtained from the patients who died of the disease (mean \pm SEM; 36 ± 8 , $n=7$) as compared with those patients who were alive (101 ± 15 , $n=25$) (Mann-Whitney U test, $p=0.043$). Then, the patients were divided into 2 groups according to the median value of *ING1* mRNA expression in the tumor. The log-rank test showed that the prognosis of the patients with decreased expression of *ING1* was significantly poor ($p=0.017$) (Table I and Fig. 2).

*The expression of *p53* was not correlated with the prognosis of neuroblastoma.* Since *ING1* has been shown to modulate the function of *p53* through the physical interaction with *p53*

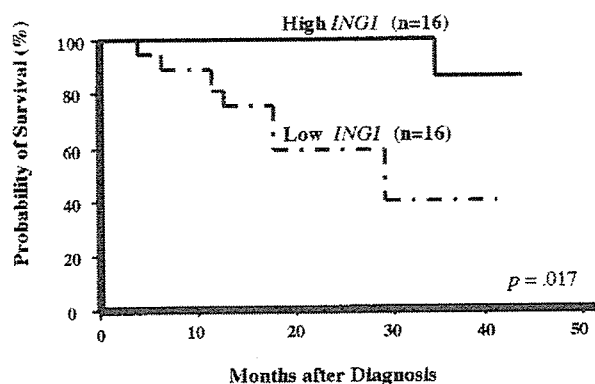


Figure 2. *ING1* mRNA expression and survival curves calculated by the Kaplan-Meier method. Kaplan-Meier life table analysis was used to compare the individual variables and survival, and different survival curves were compared using the log-rank test. Statistical analyses were performed using the StatView version 4.5 and Stata version 6.0. (—), A group of patients with high levels of *ING1* expression; (- - -), a group of patients with low levels of *ING1* expression.

Table II. Cox regression models using dichotomous factors of age, disease stage, *MYCN* amplification and expression of *Trk-A* and *ING1*.

Factor	n	p-value	HR (95% CI)
Age (≥ 1 vs. < 1 year)	31	.013	14.6 (1.75-121)
Stage (III+IV vs. I+II+IVs)	32	.069	4.6 (0.89-23.6)
<i>MYCN</i> ampl. (> 1 vs. 1 copy)	32	$< .0005$	55.8 (6.01-518)
<i>Trk-A</i> exp. (low vs. high)	30	.016	9.4 (1.53-57.8)
<i>ING1</i> exp. (low vs. high)	32	.046	9.0 (1.04-77.2)
<i>ING1</i> exp. (low vs. high)	31	.022	27.1 (1.61-455)
Age (≥ 1 vs. < 1 year)		.008	24.3 (2.32-255)
<i>ING1</i> exp. (low vs. high)	32	.023	15.7 (1.47-167)
Stage (III+IV vs. I+II+IVs)		.025	7.7 (1.30-45.2)
<i>ING1</i> exp. (low vs. high)	30	.063	12.9 (0.87-190)
<i>Trk-A</i> exp. (low vs. high)		.017	17.3 (1.68-179)

All variables with 2 categories; HR, hazard ratio shows the relative risk of death of first category relative to the second; CI, confidence interval.

(14), we also examined the expression levels of *p53* in the same neuroblastoma tissues by Northern blot hybridization. The expression of β -actin mRNA served as an internal control, and the patients were divided into 2 groups with detectable (high) and undetectable (low) expression of *p53*. As shown in Table I, *p53* expression was not significantly associated with the prognosis of neuroblastoma ($p=0.25$). These results suggest that the decreased expression of *ING1* but not of *p53* is correlated with the unfavorable prognosis of neuroblastoma.

ING1 expression is an independent prognostic indicator for neuroblastoma. We then performed a multivariate analysis of the prognostic factors for neuroblastoma including *ING1* expression. As shown in Table II, the predictive importance

of *ING1* expression for survival was demonstrated after controlling patient's age ($p=0.022$) and disease stage ($p=0.023$), whereas *ING1* expression was marginally significant ($p=0.063$) after controlling *TrkA* expression. This implied that *ING1* expression may be a prognostic indicator which is independent on age and stage, but that it may be weakly associated with *TrkA* expression in predicting the prognosis of neuroblastoma.

Discussion

In the present study, we have searched for mutations of the *ING1* gene, and examined the expression levels of *ING1* mRNA in 32 primary neuroblastoma tissues. Although we did not detect any mutations with amino acid substitutions, we found that the expression levels of *ING1* mRNA were significantly reduced in unfavorable neuroblastoma, and this marked down-regulation was associated with the poor prognosis of neuroblastoma. Our present results represent an initial step toward understanding the biological significance of *ING1* in neuroblastoma.

Recently, it has been shown that *ING1* has an ability to promote cell cycle arrest and apoptosis in certain mammalian cultured cells (14,28). Garkavtsev *et al* found a truncated form of *ING1* protein in neuroblastoma cell lines, which might be generated by a structural rearrangement or a deletion that occurred within the *ING1* gene (4). It remains unknown whether the truncated *ING1* protein retains the ability to inhibit cell cycle progression, and whether there exists a loss of function mutations of *ING1* in primary neuroblastoma, it is likely that *ING1* might act as a candidate tumor suppressor for neuroblastoma. Consistent with the recent reports showing that *ING1* is rarely mutated in human malignancies (5,29-31), our mutation analysis indicated that *ING1* is infrequently mutated in primary neuroblastomas and thus it might not function as a tumor suppressor in the classic manner (32). Note that our quantitative real-time RT-PCR analysis revealed that the expression levels of *ING1* mRNA were reduced in unfavorable neuroblastomas, and that this down-regulation was significantly correlated with the poor prognosis of neuroblastoma. Although the number of tumor samples used in this study was relatively small, the statistical significance of the traditional prognostic factors including patient's age ($p=0.001$), disease stage ($p=0.044$), *MYCN* amplification ($p<0.0001$) and *TrkA* expression ($p=0.0032$) were in good agreement with those reproducibly documented (15,33,34). Thus, our present results suggest that *ING1* expression is a novel prognostic indicator for neuroblastomas especially in advanced stages. In order to design a new therapeutic strategy against aggressive neuroblastoma, it will be necessary to clarify the molecular mechanisms of this transcriptional down-regulation of the *ING1* gene in unfavorable neuroblastoma.

There is considerable evidence that the *p53* pathway is not exclusively responsible for the genesis and/or progression of neuroblastoma. For example, *p53* is infrequently mutated in primary neuroblastomas, and wild-type *p53* is localized largely in cytoplasm of primary tumors as well as neuroblastoma-derived cell lines (35-39). In addition, our present study indicated that the expression levels of *p53* mRNA is not associated with the prognosis of neuroblastoma. On the other hand, it has been shown that *p53* plays an important

role in inducing neuronal cell death of sympathetic neurons, from which neuroblastoma originates (40). Recently, Nakagawa *et al* reported that during cisplatin-mediated cell death in neuroblastoma-derived SH-SY5Y cells, endogenous p53 accumulated at a protein level, suggesting that the p53 pathway is closely involved in DNA damage-induced neuroblastoma cell death (41). Previous studies have demonstrated that *ING1* physically interacts with p53, and thereby acts as a cofactor of p53 to enhance its ability to transactivate downstream target genes as well as to inhibit cell cycle progression (14,42). It is likely that the reduced expression of *ING1* could down-regulate the pro-apoptotic function of p53 and thereby promote neuroblastoma cell growth. To confirm this possibility, further studies are necessary.

Acknowledgements

We are grateful to S. Sakiyama and S. Ichimiya for valuable discussions, and A. Morohashi for preparing RNA. We thank Y. Nakamura and M. Nagano for assistance in quantitative RT-PCR analysis. This work was supported in part by a Grant-in-Aid from the Ministry of Health and Welfare for a New 10-Year Strategy for Cancer Control, a Grant-in-Aid from the Ministry of Health and Welfare for the Study Group for Treatment of Advanced Neuroblastoma, Uehara Foundation, and a Grant-in-Aid for Scientific Research from the Ministry of Education, Science, Sports and Culture, Japan. Masato Takahashi is an awardee of the Research Resident Fellowship from the Foundation for Promotion of Cancer Research in Japan.

References

- Bolande R: The neurocristopathies: a unifying concept of disease arising in neural crest maldevelopment. *Human Pathol* 5: 409-424, 1974.
- Brodeur GM and Nakagawara A: Molecular basis of clinical heterogeneity in neuroblastoma. *Am J Pediatr Hematol Oncol* 14: 111-116, 1992.
- Roninson IB, Gudkov AV, Holzmayer TA, Kirschling DJ, Kazarov AR, Zelnick CR, Mazo IA, Axenovich S and Thimmapaya R: Genetic suppressor elements: new tools for molecular oncology - Thirteenth Cornelius P. Rhoads Memorial Award Lecture. *Cancer Res* 55: 4023-4028, 1995.
- Garkavtsev I, Kazarov A, Gudkov A and Riabowol K: Suppression of the novel growth inhibitor p33/*ING1* promotes neoplastic transformation. *Nat Genet* 14: 415-420, 1996.
- Gunduz M, Ouchida M, Fukushima K, Hanafusa H, Etani T, Nishioka S, Nishizaki K and Shimizu K: Genomic structure of the human *ING1* gene and tumor-specific mutations detected in head and neck squamous cell carcinomas. *Cancer Res* 60: 3143-3146, 2000.
- Saito A, Furukawa T, Fukushige S, Koyama S, Hoshi M, Hayashi Y and Horii A: p24/*ING1*-ALT1 and p47/*ING1*-ALT2, distinct alternative transcripts of p33/*ING1*. *J Hum Genet* 45: 177-181, 2000.
- Motomura K, Nishisho I, Takai S, Tateishi H, Okazaki M, Yamamoto M, Miki T, Honjo T and Mori T: Loss of alleles at loci on chromosome 13 in human primary gastric cancers. *Genomics* 2: 180-184, 1988.
- Ried T, Petersen I, Holtgreve-Grez H, Speicher MR, Schrock E, du Manoir S and Cremer T: Mapping of multiple DNA gains and losses in primary small cell lung carcinomas by comparative genomic hybridization. *Cancer Res* 54: 1801-1806, 1994.
- Maestro R, Piccinin S, Doglioni C, Gasparotto D, Vukosavljevic T, Sulfaro S, Barzan L and Boiocchi M: Chromosome 13q deletion mapping in head and neck squamous cell carcinomas: identification of two distinct regions of preferential loss. *Cancer Res* 56: 1146-1150, 1996.
- Hyytinen ER, Frierson HF Jr, Boyd JC, Chung LW and Dong JT: Three distinct regions of allelic loss at 13q14, 13q21-22, and 13q33 in prostate cancer. *Genes Chromosomes Cancer* 25: 108-114, 1999.
- Garkavtsev I, Demetrick D and Riabowol K: Cellular localization and chromosome mapping of a novel candidate tumor suppressor gene (*ING1*). *Cytogenet Cell Genet* 76: 176-178, 1997.
- Zeremski M, Horrigan SK, Grigorian IA, Westbrook CA and Gudkov AV: Localization of the candidate tumor suppressor gene *ING1* to human chromosome 13q34. *Somat Cell Mol Genet* 23: 233-236, 1997.
- Garkavtsev I and Riabowol K: Extension of the replicative life span of human diploid fibroblasts by inhibition of the p33/*ING1* candidate tumor suppressor. *Mol Cell Biol* 17: 2014-2019, 1997.
- Garkavtsev I, Grigorian IA, Ossovskaya VS, Chernov MV, Chumakov PM and Gudkov AV: The candidate tumour suppressor p33/*ING1* cooperates with p53 in cell growth control. *Nature* 391: 295-298, 1998.
- Evans AE, D'Angio GJ and Randolph J: A proposed staging for children with neuroblastoma. Children's cancer study group A. *Cancer* 27: 374-378, 1971.
- Ikeda K, Nakagawara A, Yano H, Akiyama H, Tasaka H, Ueda K, Hara T, Ishii E, Ohgami H, Sera Y, *et al*: Improved survival rates in children over 1 year of age with stage III or IV neuroblastoma following an intensive chemotherapeutic regimen. *J Pediatr Surg* 24: 189-193, 1989.
- Nitschke R, Smith EI, Altshuler G, Altmiller D, Shuster J, Green A, Castleberry R, Hayes FA, Golembe B and Ducos R: Postoperative treatment of nonmetastatic visible residual neuroblastoma: a Pediatric Oncology Group study. *J Clin Oncol* 9: 1181-1188, 1991.
- Castleberry RP, Kun LE, Shuster JJ, Altshuler G, Smith IE, Nitschke R, Wharam M, McWilliams N, Joshi V and Hayes FA: Radiotherapy improves the outlook for patients older than 1 year with Pediatric Oncology Group stage C neuroblastoma. *J Clin Oncol* 9: 789-795, 1991.
- Look AT, Hayes FA, Shuster JJ, Douglass EC, Castleberry RP, Bowman LC, Smith EI and Brodeur GM: Clinical relevance of tumor cell ploidy and N-myc gene amplification in childhood neuroblastoma: a Pediatric Oncology Group study. *J Clin Oncol* 9: 581-591, 1991.
- Hirai M, Yoshida S, Kashiwagi H, Kawamura T, Ishikawa T, Kaneko M, Ohkawa H, Nakagawara A, Miwa M and Uchida K: 1q23 gain is associated with progressive neuroblastoma resistant to aggressive treatment. *Genes Chromosomes Cancer* 25: 261-269, 1999.
- Brodeur GM, Seeger RC, Schwab M, Varnus HE and Bishop JM: Amplification of N-myc in untreated human neuroblastomas correlates with advanced disease stage. *Science* 224: 1121-1124, 1984.
- Chomczynski P and Sacchi N: Single-step method of RNA isolation by acid guanidinium thiocyanate-phenol-chloroform extraction. *Anal Biochem* 162: 156-159, 1987.
- Nakagawara A, Arima M, Azar CG, Scavarda NJ and Brodeur GM: Inverse relationship between trk expression and N-myc amplification in human neuroblastomas. *Cancer Res* 52: 1364-1368, 1992.
- Heid CA, Stevens J, Livak KJ and Williams PM: Real-time quantitative PCR. *Genome Res* 6: 986-994, 1996.
- Ichimiya S, Nimura Y, Kageyama H, Takada N, Sunahara M, Shishikura T, Nakamura Y, Sakiyama S, Seki N, Ohira M, Kaneko Y, McKeon F, Caput D and Nakagawara A: p73 at chromosome 1p36.3 is lost in advanced stage neuroblastoma but its mutation is infrequent. *Oncogene* 18: 1061-1066, 1999.
- Sunahara M, Shishikura T, Takahashi M, Todo S, Yamamoto N, Kimura H, Kato S, Ishioka C, Ikawa S, Ikawa Y and Nakagawara A: Mutational analysis of p51A/TAP63gamma, a p53 homolog, in non-small cell lung cancer and breast cancer. *Oncogene* 18: 3761-3765, 1999.
- Jirtle RL: Genomic imprinting and cancer. *Exp Cell Res* 248: 18-24, 1999.
- Helbing CC, Veillette C, Riabowol K, Johnston RN and Garkavtsev I: A novel candidate tumor suppressor, *ING1*, is involved in the regulation of apoptosis. *Cancer Res* 57: 1255-1258, 1997.
- Toyama T, Iwase H, Watson P, Muzik H, Saettler E, Magliocco A, DiFrancesco L, Forsyth P, Garkavtsev I, Kobayashi S and Riabowol K: Suppression of *ING1* expression in sporadic breast cancer. *Oncogene* 18: 5187-5193, 1999.

30. Campos EI, Cheung KJ Jr, Murray A, Li S and Li G: The novel tumour suppressor gene *ING1* is overexpressed in human melanoma cell lines. *Br J Dermatol* 146: 574-580, 2002.
31. Chen B, Campos EI, Crawford R, Martinka M and Li G: Analyses of the tumour suppressor *ING1* expression and gene mutation in human basal cell carcinoma. *Int J Oncol* 22: 927-931, 2003.
32. Knudson AG Jr: Mutation and cancer: statistical study of retinoblastoma. *Proc Natl Acad Sci USA* 68: 820-823, 1971.
33. Coldman AJ, Fryer CJ, Elwood JM and Sonley MJ: Neuroblastoma: influence of age at diagnosis, stage, tumor site, and sex on prognosis. *Cancer* 46: 1896-1901, 1980.
34. Nakagawara A, Arima-Nakagawara M, Scavarda NJ, Azar CG, Cantor AB and Brodeur GM: Association between high levels of expression of the TRK gene and favorable outcome in human neuroblastoma. *N Engl J Med* 328: 847-854, 1993.
35. Vogan K, Bernstein M, Leclerc JM, Brisson L, Brossard J, Brodeur GM, Pelletier J and Gros P: Absence of p53 gene mutations in primary neuroblastomas. *Cancer Res* 53: 5269-5273, 1993.
36. Castresana JS, Bello MJ, Rey JA, Nebreda P, Queizan A, Garcia-Miguel P and Pestana A: No TP53 mutations in neuroblastomas detected by PCR-SSCP analysis. *Genes Chromosomes Cancer* 10: 136-138, 1994.
37. Hosoi G, Hara J, Okamura T, Osugi Y, Ishihara S, Fukuzawa M, Okada A, Okada S and Tawa A: Low frequency of the p53 gene mutations in neuroblastoma. *Cancer* 73: 3087-3093, 1994.
38. Kesbelava N, Zuo JJ, Chen P, Waidyaratne SN, Luna MC, Gomer CJ, Triche TJ and Reynolds CP: Loss of p53 function confers high-level multidrug resistance in neuroblastoma cell lines. *Cancer Res* 61: 6185-6193, 2001.
39. Moll UM, LaQuaglia M, Benard J and Riou G: Wild-type p53 protein undergoes cytoplasmic sequestration in undifferentiated neuroblastomas but not in differentiated tumors. *Proc Natl Acad Sci USA* 92: 4407-4411, 1995.
40. Aloyz RS, Bamji SX, Pozniak CD, Toma JG, Atwal J, Kaplan DR and Miller FD: p53 is essential for developmental neuron death as regulated by the TrkA and p75 neurotrophin receptors. *J Cell Biol* 143: 1691-1703, 1998.
41. Nakagawa T, Takahashi M, Ozaki T, Watanabe Ki K, Todo S, Mizuguchi H, Hayakawa T and Nakagawara A: Autoinhibitory regulation of p73 by Delta Np73 to modulate cell survival and death through a p73-specific target element within the Delta Np73 promoter. *Mol Cell Biol* 22: 2575-2585, 2002.
42. Takahashi M, Seki N, Ozaki T, Kato M, Kuno T, Nakagawa T, Watanabe K, Miyazaki K, Ohira M, Hayashi S, Hosoda M, Tokita H, Mizuguchi H, Hayakawa T, Todo S and Nakagawara A: Identification of the p33(*ING1*)-regulated genes that include cyclin B1 and proto-oncogene DEK by using cDNA microarray in a mouse mammary epithelial cell line NMuMG. *Cancer Res* 62: 2203-2209, 2002.

Polo-like Kinase 1 (Plk1) Inhibits p53 Function by Physical Interaction and Phosphorylation*

Received for publication, December 26, 2003, and in revised form, March 11, 2004
Published: JBC Papers in Press, March 15, 2004, DOI 10.1074/jbc.M3141S2200

Kiyohiro Ando^{‡§¶}, Toshinori Ozaki^{‡¶}, Hideki Yamamoto[‡], Kazushige Furuya[‡],
Mitsuchika Hosoda[‡], Syunji Hayashi[‡], Masahiro Fukuzawa[§], and Akira Nakagawara^{‡¶}

From the [‡]Division of Biochemistry, Chiba Cancer Center Research Institute, Chiba 260-8717, Japan and
the [§]First Department of Surgery, Nihon University School of Medicine, Tokyo 173-8610, Japan

Polo-like kinase 1 (Plk1) has an important role in the regulation of M phase of the cell cycle. In addition to its cell cycle-regulatory function, Plk1 has a potential role in tumorigenesis. Here we found for the first time that Plk1 physically binds to the tumor suppressor p53 in mammalian cultured cells, and inhibits its transactivation activity as well as its pro-apoptotic function. During the cisplatin-induced apoptosis in human neuroblastoma SH-SY5Y cells, the expression level of Plk1 was significantly decreased both at mRNA and protein levels, whereas cisplatin treatment caused a remarkable stabilization of p53. Systematic immunoprecipitation analyses using a series of deletion mutants of p53 revealed that a sequence-specific DNA-binding region of p53 is required and sufficient for the physical interaction with Plk1. The ectopically overexpressed Plk1 was co-localized with the endogenous p53 in mammalian cell nucleus, as shown by confocal laser microscopy. Expression of exogenous Plk1 and p53 in p53-deficient lung carcinoma H1299 cells greatly decreased the p53-mediated transcription from the p53-responsive *p21^{WAF1}*, *MDM2*, and *BAX* promoters, whereas the kinase-deficient mutant form of Plk1 failed to reduce the transcriptional activity of p53. Consistent with the luciferase reporter analysis, Plk1 had an ability to block the p53-dependent induction of the endogenous *p21^{WAF1}*. In addition, Plk1 inhibited the pro-apoptotic function of p53 in H1299 cells. Intriguingly, Plk1-mediated repression of p53 was attenuated with ATM. Thus, our present findings strongly suggest that p53 is a critical target of Plk1, and its function is abrogated through the physical interaction with Plk1.

The polo-like kinases (Plks)¹ are structurally and functionally related to the *Drosophila* polo serine/threonine (Ser/Thr)

* This work was supported in part by a grant-in-aid from the Ministry of Health and Welfare for a New 10-Year Strategy for Cancer Control, a grant-in-aid for Scientific Research on Priority Areas, a grant-in-aid for Scientific Research (B) from the Ministry of Education, Science, Sports and Culture, Japan, and the Hisamitsu Pharmaceutical Company. The costs of publication of this article were defrayed in part by the payment of page charges. This article must therefore be hereby marked "advertisement" in accordance with 18 U.S.C. Section 1734 solely to indicate this fact.

[¶] Both authors contributed equally to this work.

[‡] To whom correspondence should be addressed: Division of Biochemistry, Chiba Cancer Center Research Institute, 666-2 Nitona, Chuohku, Chiba 260-8717, Japan. Tel.: 81-43-264-5431; Fax: 81-43-265-4459; E-mail: akirana@chiba-ccri.chuo.chiba.jp.

¹ The abbreviations used are: Plk, polo-like kinase; ATM, ataxia telangiectasia mutated; GFP, green fluorescence protein; GST, glutathione S-transferase; NLS, nuclear localization signal; NMS, normal mouse serum; PBS, phosphate-buffered saline; TBS, Tris-buffered saline; TK, thymidine kinase; RT, reverse transcriptase.

kinase (1), and are evolutionarily well conserved from yeast to mammals. A high degree of amino acid sequence similarity is detected within a catalytic domain and a unique noncatalytic domain (termed the polo-box) located at the NH₂- and COOH-terminal region, respectively (2). It has been shown that the polo-box is critical for the correct subcellular localization of Plks (3, 4), and the COOH-terminal region containing the polo-box serves to regulate its kinase activity (5). A growing body of evidence obtained in various experimental systems suggests that Plks play an important role in the regulation of a variety of M-phase-specific events including entry into and exit from mitosis (1, 6–8). In addition to their critical role during the G₂/M transition, Plks might be also required for G₁/S phase transition (9, 10).

In mammalian cells, there exist at least three Plk family members including Plk1, Plk2, and Plk3. Plk1 (also referred to as Plk) has been identified as a serine/threonine kinase that displays an extensive amino acid sequence homology to *Drosophila* polo (2, 9, 11–13), whereas Plk2 (alternatively named Snk) and Plk3 (alternatively termed as proliferation related kinase, Prk) have been originally shown to be transcriptionally induced in response to mitogens (14, 15). In mammalian cultured cells, the amounts of Plk1 mRNA and protein are regulated in a cell cycle-dependent manner, rising from a very low level in G₁ phase to a maximal level during G₂/M phase (11, 12). The kinase activity of Plk1 is regulated by its phosphorylation and peaks at M phase (16–18). Recently, it has been shown that the kinase activity of Plk1 is inhibited in response to DNA damage in mammalian cultured cells and this inhibition occurs in an ATM-dependent manner (19, 20). Plk1 phosphorylates various substrate proteins including cyclin B1 and Cdc25C. At the onset of mitosis, Plk1 phosphorylates cyclin B1 and promoted rapid nuclear translocation of an active Cdc2-cyclin B1 complex (21, 22). In addition, Toyoshima-Morimoto *et al.* (23) has found that, during G₂/M phase, Plk1 is capable of phosphorylating Cdc25C, which dephosphorylates and directly activates the Cdc2-cyclin B1 complex, and regulating the nuclear entry of Cdc25C. In contrast to Plk1, the expression level of Plk3 remains constant during the cell cycle progression and its kinase activity peaks during late S and G₂ phase (24, 25). Xie *et al.* (26) found that the kinase activity of Plk3 is rapidly increased in response to DNA damage in an ATM-dependent fashion.

In addition to the potential cell cycle-regulatory role, Plk1 has been implicated in the genesis and/or progression of tumors. *Plk1* was overexpressed in rapidly proliferating cells as well as various human primary tumors (27), suggesting that the expression level of *Plk1* is tightly linked to proliferation and could be used as a negative prognostic indicator for various

tumors (28–30). Consistent with these observations, constitutive overexpression of *Plk1* in NIH3T3 cells resulted in the oncogenic focus formation and induction of tumor growth in nude mice (10). Down-regulation of the endogenous *Plk1* by using several antisense oligonucleotides targeted to *Plk1* induced growth inhibition in certain cancerous cells (31). Additionally, treatment of the cells with small interfering RNA targeted against *Plk1* caused the cell cycle arrest and apoptosis (32, 33). Of note, Liu and Erikson (33) reported that the tumor suppressor *p53* might be involved in the *Plk1* depletion-induced apoptosis. Recently, *Plk1* has also been reported to have an ability to phosphorylate *p53* *in vitro*, however, it is still unknown whether there exists a functional association between *Plk1* and *p53* (26). In sharp contrast to *Plk1*, the expression level of *Plk3* was significantly down-regulated in several human primary tumors including lung carcinomas and head and neck squamous cell carcinomas, as compared with their corresponding normal tissues (34, 35). Overexpression of *Plk3* in mammalian cultured cells inhibited proliferation and induced apoptosis (36). Furthermore, it has been demonstrated that *Plk3* physically interacts with *p53* and phosphorylates the Ser²⁰ of *p53*, which might result in the enhancement of its activity. These suggest that *Plk1* and *Plk3* play a differential role in regulating cell proliferation and oncogenesis, and that *p53* participates in *Plk3*-dependent growth inhibition and/or apoptosis (25, 26, 36, 37).

In the present study, we examined the physical and functional interaction between *Plk1* and *p53*. We found that *Plk1* binds to the sequence-specific DNA-binding domain of *p53*, and inhibits the *p53*-dependent transcriptional activation as well as pro-apoptotic function. Intriguingly, overexpression of ATM abrogated the *Plk1*-mediated inhibitory effect on *p53*. These results suggest that the *Plk1*-mediated negative regulation of *p53* might be a fundamental mechanism for the *Plk1*-induced oncogenesis.

EXPERIMENTAL PROCEDURES

Tumor Samples—Surgically resected tumor tissues including three lung adenocarcinomas, two gastric adenocarcinomas, one uterus carcinoma, two bladder carcinomas, and their corresponding normal tissues used in this study were obtained as frozen specimens from the Tissue Bank in Chiba Cancer Center Hospital (Chiba, Japan). Six hepatoblastomas and their matched normal tissues were provided by the Japanese Study Group for Pediatric Liver Tumor.

Cell Culture—African green monkey kidney COS7 cells were maintained in Dulbecco's modified Eagle's medium supplemented with 10% heat-inactivated fetal bovine serum (Invitrogen) and penicillin (100 IU/ml)/streptomycin (100 µg/ml). Human neuroblastoma SH-SY5Y cells and human lung carcinoma H1299 cells were grown in RPMI 1640 medium containing 10% heat-inactivated fetal bovine serum and antibiotic mixture. Cultures were maintained at 37 °C in a water-saturated atmosphere of 5% CO₂ in air.

Transfection—COS7 cells were transfected with the indicated expression plasmids using FuGENE 6 transfection reagent (Roche Applied Science) in a 6-cm diameter culture dish in accordance with the manufacturer's specifications. Transfection of H1299 cells was conducted by lipofection with LipofectAMINE transfection reagent (Invitrogen) in a 12-well plate according to the manufacturer's instructions.

RT-PCR—Total RNA was prepared from SH-SY5Y cells exposed to cisplatin by using the RNeasy Mini Kit (Qiagen Inc., Valencia, CA) according to the manufacturer's protocol, and subjected to synthesis of the first strand cDNA with random primers and a SuperScript II reverse transcriptase (Invitrogen) at 42 °C for 1 h. When the reaction was complete, the cDNA was amplified in a final volume of 15 µl of reaction mixture containing 100 µM of each deoxynucleoside triphosphate, 1× PCR buffer, 1 µM of each primer, and 0.2 units of rTaq DNA polymerase (Takara, Ohtsu, Japan). The primers for *p53* amplification were 5'-ATTGATGCTGTCCCGGACGATATTGAAC-3' and 5'-ACCTTTTGGACTTCAGGTGCTGGAGTG-3'. The primers for *p21^{WAF1}* amplification were 5'-ATGAAATTCACCCCTTTCC-3' and 5'-CCCTAGCTGTCTCACTC-3'. The primers for *Plk1* amplification were 5'-ATCACCTGCCTGACCATTCCACCAAGG-3' and 5'-AATTGCGGAAA-

TATTTAAGGAGGGTGATCT-3'. The primers for *Plk3* amplification were 5'-CGCGAGAAGATCCTAAATG-3' and 5'-GATCTGCCGAGGTAGTAGC-3'. The primers for *GAPDH* amplification were 5'-ACCTGACCTGCCGTCTAGAA-3' and 5'-TCCACCACCCTGTTGCTGTA-3'. The PCR-amplified products were separated by electrophoresis on a 1.5% agarose gel and visualized by ethidium bromide post-staining.

Generation of FLAG-tagged Expression Constructs—The FLAG-tagged human *Plk1* construct was generated by PCR amplification using the cDNA derived from primary hepatoblastoma as a template. The forward and reverse primers used in the PCR were 5'-CCGCTCCAGAGTGTCTGACTGACTGCAGGGAAG-3' and 5'-CTAGTCTAGATTAGGAGCCTTGAGACGGTTCCT-3'. The underlined nucleotides represent the XhoI restriction sites in the forward primer and the XbaI restriction site in the reverse primer. The PCR product was subcloned into pGEM-T Easy (Promega Corp., Madison, WI), and its nucleotide sequence was verified by automated dideoxy terminator cycle sequencing. The PCR product was digested with XhoI and XbaI, and inserted between the XhoI to XbaI sites in the pcDNA3-FLAG expression plasmid in-frame to the downstream of the FLAG tag to give pcDNA3-FLAG-*Plk1*.

Construction of the Deletion Mutants of *p53* and *Plk1*—The *p53* deletion mutants, *p53*-(1–359), *p53*-(1–292), and *p53*-(1–101) were generated by using the forward primer 5'-CCCAGCTTGGGATGGAGGAGCCGACGTGATCCTAGCGTC-3' (1F) in combination with the reverse primers 5'-CCGGAATTCGGTTCATGGCTCCTCCAGCCTGGGCATCCTT-3' (359R), 5'-CCGGAATTCGGTTCATTTCTTGGGAGATTCTCTTCTCTGT-3' (292R) and 5'-CCGGAATTCGGTTCATTTCTGGGAAGGGACAGAAGATGACA-3' (101R), respectively. *p53*-(102–393) was amplified by using the forward primer 5'-CCCAGCTTGGGATGACCTACCAGGGCAGCTACGGTTTCCGTCT-3' (102F) and the reverse primer 5'-CCGGAATTCGGTTCAGTCTGAGTCAGGCCCTTCTGTCTGAACAT-3' (393R). Each of the forward and reverse primers contained the HindIII and EcoRI restriction sites to facilitate the subsequent cloning step. Underlined nucleotides in the oligonucleotides listed above were HindIII or EcoRI sites. Amplified fragments were digested with HindIII and EcoRI, and subcloned directly into the identical restriction sites of pcDNA3 to give pcDNA3-*p53*-(1–359), pcDNA3-*p53*-(1–292), pcDNA3-*p53*-(1–101), and pcDNA3-*p53*-(102–393). All of the constructs were confirmed by sequence analysis. For the construction of the deletion mutants of *Plk1*, pcDNA3-FLAG-*Plk1* was digested with BamHI, BamHI and BstXI, or BamHI and NcoI. A restriction fragment encoding amino acid residues 1–401, 1–329, or 1–98 was purified from agarose gels, filled in the overhangs with Klenow, and then inserted in-frame into the enzymatically modified BamHI and XhoI sites of the pcDNA3-FLAG expression plasmid to give pcDNA3-FLAG-*Plk1*-(1–401), pcDNA3-FLAG-*Plk1*-(1–329), or pcDNA3-FLAG-*Plk1*-(1–98), respectively. DNA sequencing confirmed the authenticity of the expression plasmids prior to transfection.

Construction of the Kinase-deficient Mutant Form of *Plk1*—The K82M mutation was introduced into wild-type *Plk1* by the PCR-based strategy using *PfuUltra*™ High Fidelity DNA polymerase (Stratagene, La Jolla, CA) according to the manufacturer's instructions. The following oligonucleotides were used: 5'-ATGATTGTGCTAAGTCTCTGCTGCTCAAGCCGCA-3' (underlined segment encodes Met at amino acid position 82) and 5'-GCCCGCAACACCTCCTTGGTGTCCGCTCCGAGA-3'. Nucleic acid sequencing was performed to verify the presence of the desired mutation and absence of random mutations. The amplified fragment that contains the K82M mutation was then digested with HindIII and NcoI, gel-purified, and ligated with the NcoI/XbaI restriction fragment containing the 3'-portion of the wild-type *Plk1* cDNA. The resulting entire cDNA encoding the full-length *Plk1* carrying the amino acid substitution at position 82 was inserted in-frame into the HindIII and XbaI sites of the pcDNA3-FLAG expression plasmid to give pcDNA3-FLAG-*Plk1*(K82M).

Construction of the Expression Plasmid for Antisense *Plk1*—A full-length human *Plk1* cDNA was ligated into the pcDNA3 expression plasmid in a reverse orientation to give As-*Plk1*, and the product was evaluated by restriction digestion. To assess the effect of As-*Plk1* on the endogenous *Plk1*, whole cell lysates prepared from H1299 cells transfected with As-*Plk1* were analyzed for *Plk1* by immunoblotting.

GST Pull-down Assay—Whole cell lysates prepared from COS7 cells expressing FLAG-*Plk1* were incubated with 1 µg of GST or GST-*p53* (Santa Cruz Biotechnologies, Santa Cruz, CA) immobilized on glutathione-Sepharose beads for 2 h at 4 °C. The beads were washed extensively with NETN buffer (50 mM Tris-Cl, pH 7.5, 150 mM NaCl, 0.1% Nonidet P-40, and 1 mM EDTA) containing 1 mM phenylmethylsulfonyl fluoride. The bound proteins were eluted with 2× SDS sample buffer by boiling

for 5 min, and separated by 10% SDS-polyacrylamide gel electrophoresis followed by immunoblotting.

Immunofluorescent Labeling and Confocal Microscopy—COS7 cells, cultured onto glass coverslips, were transiently transfected with the expression plasmid for FLAG-Plk1. Transfected cells were washed twice with 1× PBS and then fixed with 1× PBS containing 3.7% formaldehyde for 30 min at room temperature. After washing with 1× PBS, cells were permeabilized with 0.2% Triton X-100 for 5 min at room temperature and blocked for 1 h in 1× PBS containing 3% bovine serum albumin. Cells were then incubated with polyclonal anti-p53 antibody (Cell Signaling Technology, Inc., Beverly, MA) and monoclonal anti-FLAG antibody (M2, Sigma) for 1 h at room temperature. After incubation with primary antibodies, cells were washed twice with 1× PBS and incubated with fluorescein isothiocyanate- or rhodamine-conjugated secondary antibodies (Invitrogen) diluted 1:200 for 1 h at room temperature. Cell nuclei were stained with 4,6-diamidino-2-phenylindole at a final concentration of 1 μg/ml (Sigma). Cells were finally washed with 1× PBS, the coverslips were removed from the dishes, mounted onto slides, and observed under Fluoview laser scanning confocal microscope (Olympus, Tokyo, Japan).

Western Blot Analysis—Cells were transfected with the indicated combinations of the expression plasmids. Forty-eight hours after transfection, cells were extracted directly with the lysis buffer containing 25 mM Tris-HCl, pH 8.0, 137 mM NaCl, 2.7 mM KCl, 1% Triton X-100, 1 mM phenylmethylsulfonyl fluoride and protease inhibitor mixture (Sigma) and the whole cell lysates were sonicated for 10 s followed by centrifugation at 15,000 rpm for 10 min at 4 °C to remove insoluble materials. The protein concentrations were determined using the Bradford protein assay according to the instructions of the vendor (Bio-Rad). Equal amounts of the whole cell lysates (50 μg of protein) were boiled in an SDS sample buffer consisting of 62.5 mM Tris-HCl, pH 6.8, 2% SDS, 2% β-mercaptoethanol, and 0.01% bromophenol blue and subjected to 10% SDS-polyacrylamide gel electrophoresis under reducing conditions and then electrotransferred onto Immobilon-P membranes (Millipore, Bedford, MA) at room temperature for 1 h. The membranes were blocked with TBS-T (50 mM Tris-Cl, pH 7.6, 100 mM NaCl, and 0.1% Tween 20) containing 5% nonfat dry milk at room temperature for 1 h, and subsequently incubated for 1 h with monoclonal anti-Plk1 (PL2 and PL6, Zymed Laboratories, Inc., San Francisco, CA), monoclonal anti-p53 (DO-1, Oncogene Research Products, Cambridge, MA), monoclonal anti-FLAG antibody (M2, Sigma), monoclonal anti-Plk3 antibody (B37-2, BD Pharmingen), polyclonal antibody specific for p53 phosphorylated at Ser¹⁵ (Cell Signaling, Beverly, MA), polyclonal anti-p21^{WAF1} antibody (H-164, Santa Cruz Biotechnologies), or polyclonal anti-actin antibody (20-33, Sigma) in TBS-T, followed by an incubation with horseradish peroxidase-conjugated goat anti-mouse or anti-rabbit secondary antibody (Jackson ImmunoResearch Laboratories, West Grove, PA) diluted at 1:2,000 for 1 h at room temperature. The membranes were washed extensively with TBS-T and protein bands were visualized by enhanced chemiluminescence (ECL) according to the manufacturer's instructions (Amersham Biosciences).

Subcellular Fractionation—Cells were fractionated into cytosolic and nuclear fractions as described previously (38). Briefly, cells were washed twice with ice-cold 1× PBS and lysed in lysis buffer containing 10 mM Tris-HCl, pH 7.5, 1 mM EDTA, 0.5% Nonidet P-40, and a protease inhibitor mixture (Sigma) for 30 min at 4 °C. Cell lysates were centrifuged at 15,000 × *g* for 10 min to collect the soluble fraction as cytosolic extracts. Insoluble materials were washed with the lysis buffer and further dissolved in 1× SDS sample buffer to collect the nuclear fraction. The nuclear and cytoplasmic fractions were subjected to immunoblot analysis using the anti-FLAG, monoclonal anti-lamin B (Ab-1, Oncogene Research Products), or monoclonal anti-Ras (RASK-3, Seikagaku Co., Tokyo, Japan) antibody.

Immunoprecipitation and Western Blot Analysis—For the immunoprecipitation of Plk1 and p53, COS7 cells were transiently transfected with 2 μg of the expression plasmid for FLAG-Plk1 using FuGENE 6 transfection reagent. Forty-eight hours post-transfection, cells were harvested and lysed by incubation with mixing in 400 μl of the EBC buffer (50 mM Tris-HCl, pH 7.5, 120 mM NaCl, 0.5% Nonidet P-40, and 1 mM phenylmethylsulfonyl fluoride) at 4 °C for 30 min. Whole cell lysates were then subjected to centrifugation at 15,000 × *g* for 20 min at 4 °C to remove insoluble materials. Equal amounts of whole cell lysates were precleared with 30 μl of a 50% slurry of protein A-Sepharose (Amersham Biosciences). After centrifugation, the supernatant was incubated with the normal mouse serum (NMS), monoclonal anti-FLAG, or monoclonal anti-p53 antibody at 4 °C for 2 h. The immunocomplexes were precipitated with the protein A-Sepharose beads at 4 °C for 30 min, which were then pelleted by centrifugation at 15,000 × *g* for

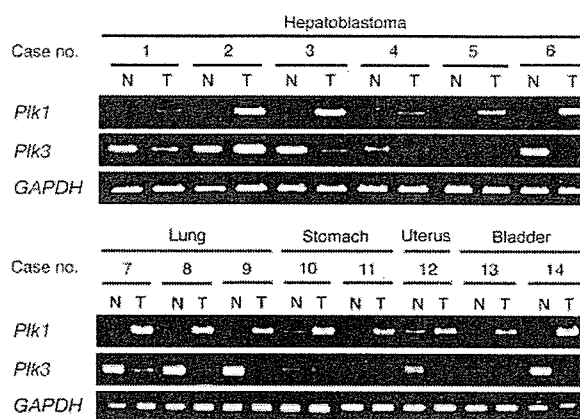


FIG. 1. Expression of *Plk1* and *Plk3* mRNA in various human primary tumors and their corresponding normal tissues. Total RNA (5 μg) prepared from the indicated tumor (T)-normal (N) paired samples was subjected to RT-PCR analysis for *Plk1* and *Plk3* mRNA expression using the specific primers as shown under "Experimental Procedures." The PCR-amplified products were analyzed by 1.5% agarose gel electrophoresis and visualized by ethidium bromide staining. Amplification of *GAPDH* was used as an internal control.

5 min. The precipitates were washed with the lysis buffer three times at 4 °C, resuspended in 30 μl of the SDS sample buffer, and treated at 100 °C for 5 min. Proteins were then resolved by 10% SDS-polyacrylamide gel electrophoresis, and transferred onto the Immobilon-P membranes. The protein complex was detected by Western blot analysis using the monoclonal anti-FLAG or monoclonal anti-p53 antibodies.

Luciferase Reporter Assays—p53-deficient H1299 cells were seeded in a 12-well tissue culture dish at a density of 5×10^4 cells/well. Cells were transfected with 100 ng of the p53-responsive luciferase reporter plasmid (*p21*, *MDM2*, or *BAX*), 10 ng of pRL-TK *Renilla* luciferase cDNA, and 25 ng of the expression plasmid for p53 together with or without increasing amounts of FLAG-Plk1 expression plasmid. The total amount of DNA was kept constant (510 ng) with pcDNA3 (Invitrogen) per transfection. Forty-eight hours post-transfection, transfected cells were washed twice with 1× PBS, and resuspended in passive lysis buffer (Promega Corp.). Both firefly and *Renilla* luciferase activities were assayed with the dual-luciferase reporter assay system (Promega Corp.) according to the manufacturer's instructions. The fluorescent light emission was determined by TD-20 luminometer (Turner Design, Sunnyvale, CA). The firefly luminescence signal was normalized based on the *Renilla* luminescence signal. The results were obtained from at least three sets of transfection and were presented as the mean ± S.D.

Cell Survival Assays—Cell viability was determined by a modified 3-(4,5-dimethylthiazol-2-yl)-2,5-diphenyltetrazolium bromide (MTT) assay. In brief, SH-SY5Y cells were seeded in 96-well microtiter plates (5×10^3 cell/well) with 100 μl of complete medium and allowed to attach. The next day, the medium were changed and cells were treated with cisplatin for 24 h. For the MTT assay, 10 μl of MTT solution was added to each well for 3 h at 37 °C. The absorbance readings for each well were carried out at 570 nm using the microplate reader (model 450, Bio-Rad).

Apoptotic Analysis—H1299 cells were transfected with a constant amount of the expression plasmid for green fluorescence protein (GFP) and p53 expression plasmid together with or without the expression plasmid encoding FLAG-Plk1. Forty-eight hours after transfection, transfected cells were identified by the presence of green fluorescence. To verify apoptosis, cell nucleus was stained with propidium iodide to reveal nuclear condensation and fragmentation. The number of GFP-positive cells with fragmented nuclei was scored, and presented as a percentage of the total number of fluorescent cells.

RESULTS

Expression of *Plk1* and *Plk3* in Paired Tumors and Adjacent Normal Tissues—It has been shown that the expression level of *Plk1* is increased in human tumors of various origins as compared with that of their corresponding normal tissues, suggesting that Plk1 contributes to the genesis and/or progression of tumors (13, 27–29). Recently, we have also identified *Plk1* as

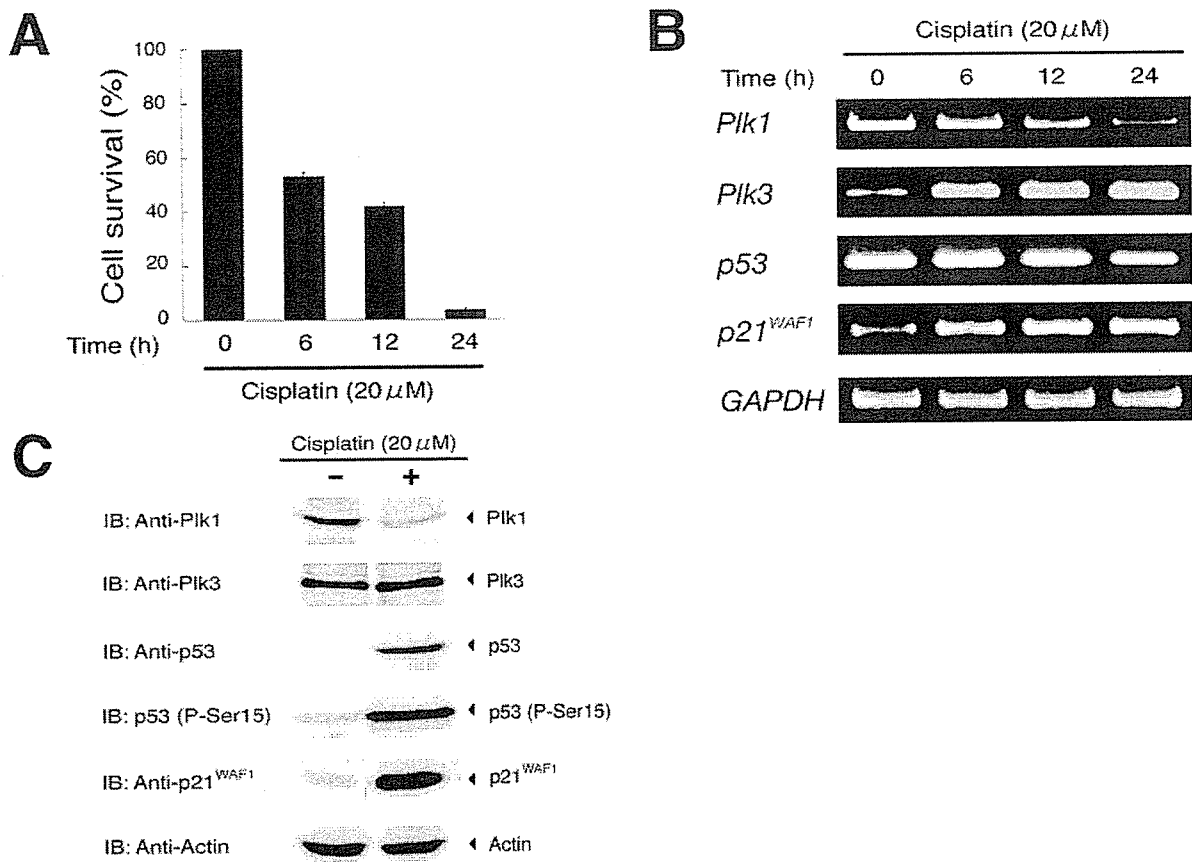


FIG. 2. Down-regulation of *Plk1* during the cisplatin-induced apoptosis. **A**, cell survival assays of SH-SY5Y cells treated with cisplatin. SH-SY5Y cells were exposed to cisplatin at a final concentration of 20 μM . At the indicated time periods after treatment with cisplatin, cell viability was determined by MTT assay. Data are presented as the mean \pm S.D. of three independent experiments. **B**, RT-PCR analysis. Human neuroblastoma-derived SH-SY5Y cells were treated with or without cisplatin at a final concentration of 20 μM . At the indicated time periods after treatment with cisplatin, total RNA was prepared and subjected to RT-PCR analysis for the expression of *Plk1* (1st panel), *Plk3* (2nd panel), *p53* (3rd panel), and *p21^{WAF1}* (4th panel). Amplification of *GAPDH* serves as an internal control (5th panel). The PCR products were resolved in 1.5% agarose gels and visualized by ethidium bromide staining. **C**, Western blot analysis. Whole cell lysates were prepared from SH-SY5Y cells exposed to cisplatin for 24 h (at a final concentration of 20 μM) or left untreated and immunoblotted against anti-*Plk1* (1st panel), anti-*Plk3* (2nd panel), anti-*p53* (3rd panel), antibody specific for *p53* phosphorylated at Ser¹⁵ (4th panel), or with the anti-*p21^{WAF1}* antibody (5th panel). Immunoblotting for actin is shown as control for protein loading (6th panel).

one of the genes whose expression level is markedly elevated in human hepatoblastomas.² In contrast, *Plk3* expression is down-regulated in certain human tumors including lung carcinomas and head and neck squamous cell carcinomas (34, 35). To confirm the differential expression of both *Plk1* and *Plk3* in the same tissue samples, we examined their expression patterns among the indicated various paired cancer-normal tissues by RT-PCR. The levels of *GAPDH* mRNA were comparable between these paired samples. Consistent with the previous results, without exceptions, the expression levels of *Plk1* mRNA were significantly higher in cancerous tissues than those of their adjacent normal tissues (Fig. 1). On the other hand, *Plk3* was expressed at low levels in all the lung, uterus, and bladder carcinomas that we examined, as compared with their corresponding normal tissues, whereas a significant decrease in *Plk3* expression level in tumor tissues was undetectable in 2 of 6 hepatoblastomas and in 1 of 2 gastric carcinomas (Fig. 1). Thus, deregulated overexpression of *Plk1* is detected in all various types of tumors, whereas down-regulation of *Plk3* expression may be restricted to certain tumors.

Cisplatin Treatment Induces Down-regulation of *Plk1* in Association with Up-regulation of *p53* in SH-SY5Y Cells—To analyze whether *Plk1* expression could be modulated during the cisplatin-induced apoptosis, whole cell lysates and total RNA were prepared from human neuroblastoma-derived SH-SY5Y cells after treatment with or without cisplatin, and were subjected to immunoblot analysis and RT-PCR, respectively. In accordance with our previous observations (39), cells underwent apoptosis in a time-dependent manner as measured by the cell survival assay (Fig. 2A), and a remarkable stabilization of *p53* at the protein level was detected after treating the cells with cisplatin, accompanied with a significant up-regulation of *p21^{WAF1}* both at protein and mRNA levels (Fig. 2, B and C). In addition to the increase in the level of total *p53*, the phosphorylation of *p53* at Ser¹⁵ was dramatically enhanced in cells exposed to cisplatin, whereas that of *p53* at Ser²⁰ was undetectable (data not shown). Intriguingly, cisplatin treatment markedly reduced the expression level of *Plk1* mRNA and protein (Fig. 2, B and C), suggesting that there exists an inverse relationship between the expression levels of *p53* and *Plk1* during DNA damage-induced apoptosis. Thus, *Plk1* may play an important role in the *p53* pathway. On the other hand, cisplatin treatment resulted in a significant up-regulation of *Plk3* mRNA expression in a time-dependent manner, however,

² Yamada, S., Ohira, M., Horie, H., Ando, K., Takayasu, H., Suzuki, Y., Sugano, S., Hirata, T., Goto, T., Matsunaga, T., Hiyama, E., Hayashi, Y., Ando, H., Suita, S., Kaneko, M., Sakaki, F., Hashizume, K., Ohnuma, N., and Nakagawara, A. (2004) *Oncogene*, in press.

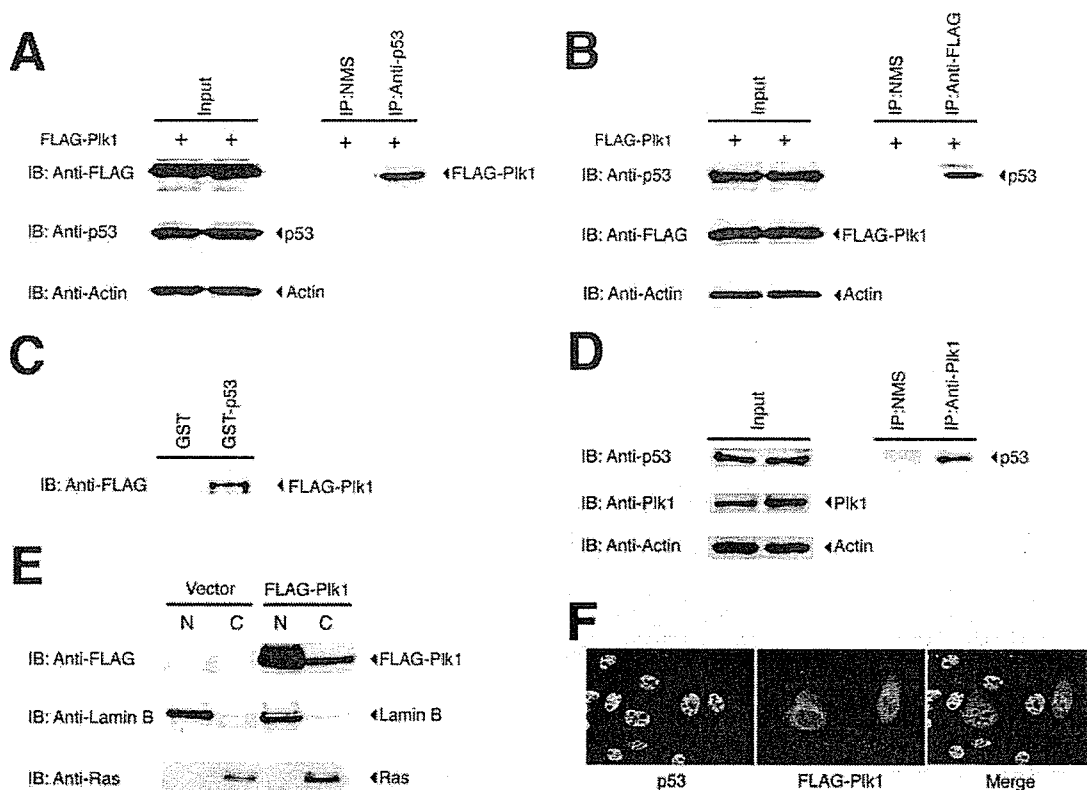


FIG. 3. Co-immunoprecipitation and nuclear co-localization of Plk1 and p53. *A*, complex formation between Plk1 and p53 in mammalian cultured cells. COS7 cells were transiently transfected with the expression plasmid for FLAG-tagged Plk1. Forty-eight hours after transfection, whole cell lysates were prepared and immunoprecipitated (IP) with NMS or with monoclonal anti-p53 antibodies. The immunocomplexes were resolved by 10% SDS-polyacrylamide gel electrophoresis and immunoblotted (IB) with monoclonal anti-FLAG antibody. Whole cell lysates were immunoblotted with monoclonal anti-p53, or with monoclonal anti-FLAG antibody to show the expression of endogenous p53, or FLAG-Plk1, respectively. The p53 blot was reprobed for actin to ensure equal loading. *B*, a similar immunoprecipitation assay was performed with NMS or monoclonal anti-FLAG antibody, followed by immunoblotting with monoclonal anti-p53 antibody. Whole cell lysates were monitored on immunoblot for the expression of endogenous p53 or FLAG-Plk1. The p53 blot was reprobed for actin to ensure equal loading. *C*, GST pull-down assay. Whole cell lysates prepared from COS7 cells expressing FLAG-Plk1 were incubated with GST or GST-p53 immobilized on glutathione-Sepharose beads. The bound proteins were separated by 10% SDS-polyacrylamide gel electrophoresis, and subjected to immunoblotting with the anti-FLAG antibody. *D*, association between endogenous p53 and Plk1. Cell lysates prepared from U2OS cells were immunoprecipitated with NMS or with monoclonal anti-Plk1 antibody, and the anti-Plk1 immunoprecipitates were immunoblotted with monoclonal anti-p53 antibody. *E*, subcellular localization of Plk1. COS7 cells were transiently transfected with the expression plasmid encoding FLAG-Plk1. Forty-eight hours after transfection, cells were fractionated into nuclear (N) and cytosolic (C) fractions as described under "Experimental Procedures." Equal amounts of each fraction were resolved by 10% SDS-polyacrylamide gel electrophoresis and immunoblotted with monoclonal anti-FLAG antibody (top panel). These extracts were also immunoblotted with monoclonal antibody specific for lamin B (middle panel) or Ras (RASK-3) (bottom panel) to show the validity of our fractionation technique. *F*, nuclear co-localization of Plk1 and p53. COS7 cells were transiently transfected with the FLAG-Plk1 expression plasmid. Following transfection, cells were fixed and incubated with polyclonal anti-p53 and monoclonal anti-FLAG antibodies that were revealed by fluorescein isothiocyanate-conjugated anti-rabbit IgG (green) and rhodamine-conjugated anti-mouse IgG (red), respectively. Merge analysis (yellow) showed the nuclear co-localization of Plk1 and p53.

the amount of Plk3 protein remained constant, regardless of cisplatin treatment.

Interaction of Plk1 with p53—Recently, it has been shown that Plk3 interacts with p53 and is directly involved in the stress-induced phosphorylation of p53 on the serine 20 residue (25, 26, 36, 37). Of note, Xie *et al.* (26) found that Plk1 is able to phosphorylate p53 *in vitro*, however, its functional significance *in vivo* remains unclear. These observations prompted us to investigate possible interactions between Plk1 and p53. For this purpose, COS7 cells, which express a large amount of endogenous p53 (40), were transiently transfected with the expression plasmid for FLAG-tagged Plk1. Whole cell lysates prepared from the transfected cells were immunoprecipitated with NMS or with a monoclonal anti-p53 antibody, and the immunoprecipitates were analyzed by immunoblotting with a monoclonal anti-FLAG antibody. As shown in Fig. 3A, FLAG-Plk1 was co-immunoprecipitated with the endogenous p53, but not present in the control immunoprecipitates obtained with the normal mouse serum. The expression of FLAG-Plk1 and

the endogenous p53 was confirmed by immunoblot analysis with the antibody against the FLAG epitope and p53, respectively (Fig. 3A). Analysis of the anti-FLAG immunoprecipitates also revealed that p53 is co-immunoprecipitated with FLAG-Plk1 (Fig. 3B). To confirm their interaction *in vitro*, GST pull-down experiments were performed using GST fusion full-length human p53. As shown in Fig. 3C, mammalian expressed FLAG-Plk1 bound to GST-p53 but not to GST alone. Their interaction was further examined using endogenous materials. Whole cell lysates prepared from U2OS cells that carry wild-type p53 (41) were immunoprecipitated with a monoclonal anti-Plk1 antibody and the anti-Plk1 immunoprecipitates were analyzed for the presence of the endogenous p53. As shown in Fig. 3D, the endogenous p53 was co-immunoprecipitated with the endogenous Plk1. Similar results were also obtained in HeLa cells (data not shown). These results clearly demonstrate that Plk1 interacts with p53 in mammalian cultured cells and *in vitro*.

To evaluate the subcellular localization of Plk1, we per-

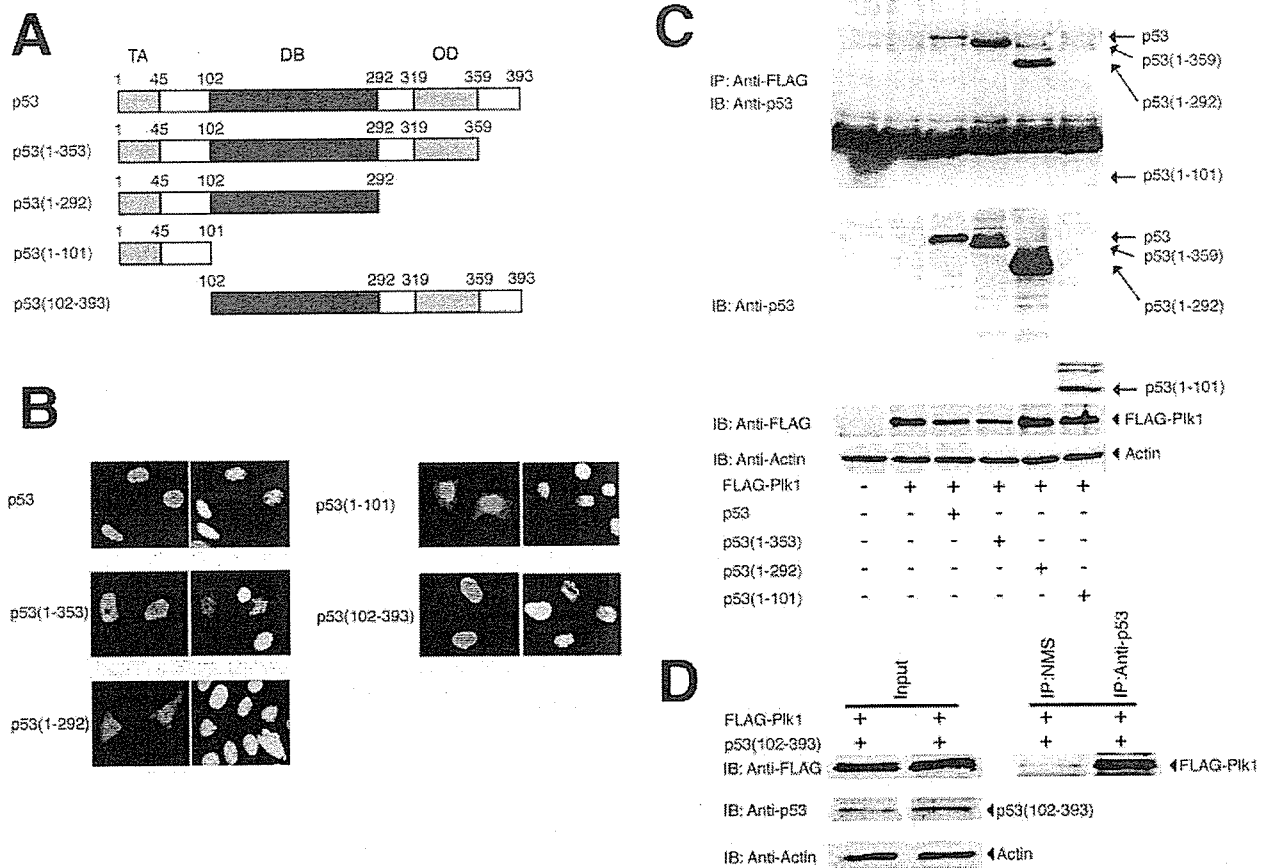


FIG. 4. DNA-binding domain of p53 is required for interaction with Plk1. *A*, schematic drawing of full-length p53 and various deletion mutants used in this study. *TA*, transactivation domain; *DB*, sequence-specific DNA-binding domain; *OD*, oligomerization domain. *Numbers* indicate amino acid position. *B*, subcellular localization of various deletion mutants of p53. p53-deficient H1299 cells were transiently transfected with the indicated expression plasmids. Forty-eight hours after transfection, cells were fixed and incubated with monoclonal anti-p53 antibody (DO-1 or PAb 421). Cell nuclei were stained with 4,6-diamidino-2-phenylindole (blue). Expression of p53 derivatives was visualized with rhodamine-conjugated secondary antibody (red). *C* and *D*, Plk1 interacts with the DNA-binding domain of p53. H1299 cells were transiently co-transfected with the indicated combinations of the expression plasmids. Forty-eight hours after transfection, whole cell lysates were prepared and subjected to immunoprecipitation with monoclonal anti-FLAG antibody followed by immunoblotting with monoclonal anti-p53 antibody (*upper panel*). The *lower panels* show the direct immunoblot analyses of whole cell lysates performed with monoclonal anti-p53, monoclonal anti-FLAG, or with polyclonal anti-actin antibody (*C*). Whole cell lysates from H1299 cells overexpressing FLAG-Plk1 and p53(102-393) were immunoprecipitated with monoclonal anti-p53 antibody (PAb421) or with NMS followed by immunoblotting with monoclonal anti-FLAG antibody. Expression levels of p53(102-393), FLAG-Plk1, and actin were examined by immunoblotting (*D*).

formed indirect immunofluorescent staining as well as biochemical cell fractionation of the transfected COS7 cells. COS7 cells transfected with the empty plasmid or with the expression plasmid for FLAG-Plk1 were fractionated into cytoplasmic and nuclear fractions for immunoblot analysis of FLAG-Plk1. Ras and lamin B served as markers for the purity of cytoplasmic and nuclear fractions, respectively (Fig. 3E, lower panels). Consistent with previous observations (10, 22, 42), FLAG-Plk1 was detected both in the cytoplasm and nucleus (Fig. 3E, upper panel). For immunofluorescent staining, COS7 cells expressing FLAG-Plk1 were fixed and stained with monoclonal anti-FLAG and polyclonal anti-p53 antibodies. As shown in Fig. 3F, FLAG-Plk1 localized to both the cytoplasm and nucleus. Merging analysis by confocal microscopy showed that FLAG-Plk1 colocalizes with endogenous p53 in cell nucleus.

The Sequence-specific DNA-binding Region of p53 Is Required for the Interaction with Plk1—To assess regions of p53 involved in the interaction with Plk1, we constructed a series of p53 deletion mutants including p53(1-359) (lacking an extreme COOH-terminal region), p53(1-292) (lacking the most COOH-terminal region including an oligomerization domain), p53(1-101) (retaining only an NH₂-terminal transactivation

domain), and p53(102-393) (lacking an NH₂-terminal transactivation domain) (Fig. 4A). We first examined their subcellular localization by indirect immunofluorescent staining. To this end, p53-deficient human lung carcinoma H1299 cells (43) were transiently transfected with each expression plasmid. Forty-eight hours after transfection, cells were fixed and stained with the appropriate monoclonal anti-p53 antibody. As described previously (44, 45), there exist three potential nuclear localization signals (NLS I, II, and III) in the COOH-terminal region of p53, and NLS I alone has an ability to translocate the pyruvate kinase fusion protein to the nucleus. As shown in Fig. 4B, wild-type p53 and p53(102-393), which retain the intact COOH-terminal region, accumulated in the nucleus. In addition, p53(1-359), which lacks the NLS II and III but retains the NLS I, localized largely in the nucleus. On the other hand, p53(1-292) and p53(1-101), which lack three potential NLSs, were detected both in the nucleus and the cytoplasm. We then examined their abilities to interact with Plk1. H1299 cells were transiently co-transfected with the FLAG-Plk1 expression plasmid along with the expression plasmid for wild-type p53, p53(1-359), p53(1-292), or p53(1-101), and the anti-FLAG immunoprecipitates were analyzed for the presence of wild-

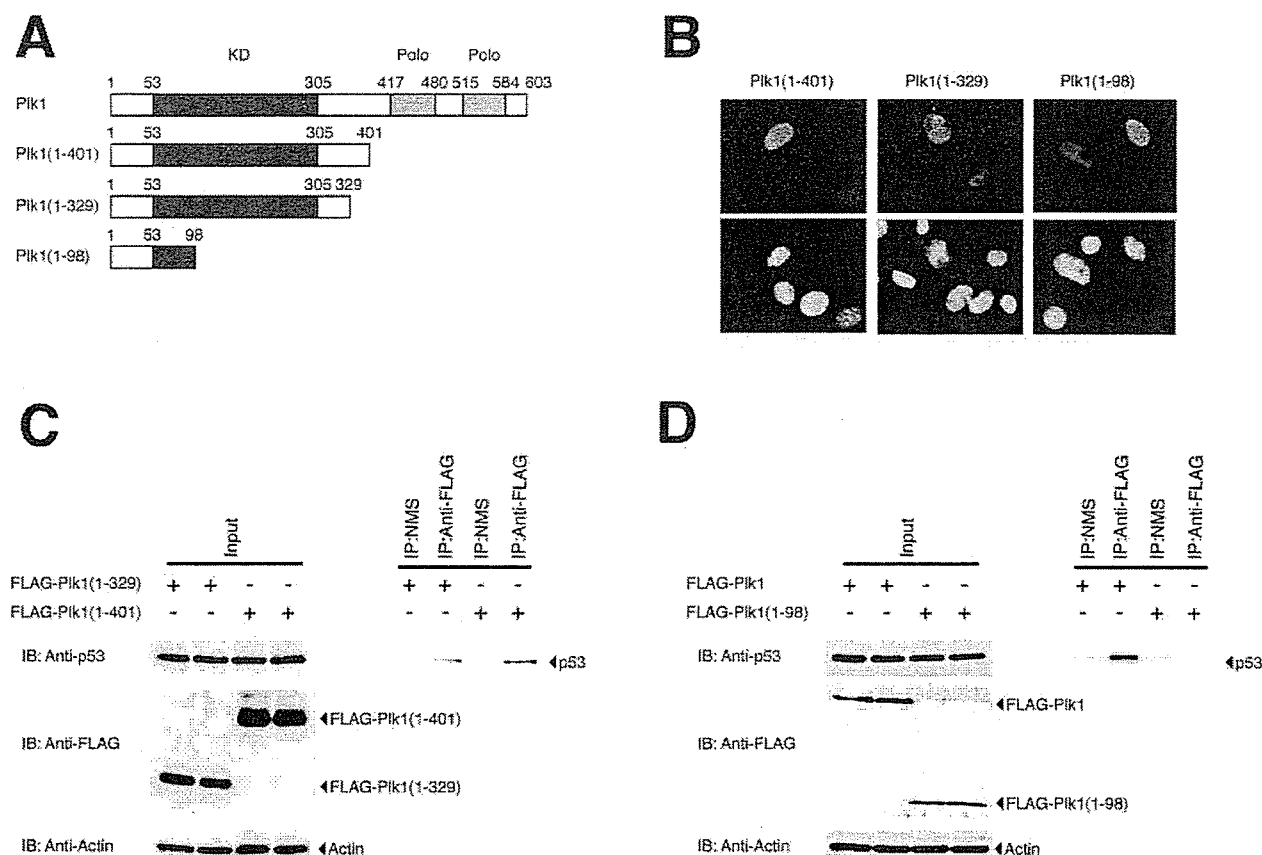


FIG. 5. Mapping of the region of Plk1 required for interaction with p53. *A*, schematic representation of Plk1 deletion mutants. *KD*, kinase domain; *Polo*, polo-box. *Numbers* indicate amino acid position. *B*, immunofluorescent studies of Plk1 deletion mutants. Transfected COS7 cells were fixed in 3.7% formaldehyde for 30 min, permeabilized with 0.2% Triton X-100 for 5 min, and blocked in PBS containing 3% bovine serum albumin for 1 h. Cells were then incubated with monoclonal anti-FLAG antibody followed by incubation with rhodamine-conjugated secondary antibody (red), and analyzed by confocal microscopy. Cell nuclei were stained with 4,6-diamidino-2-phenylindole (blue). *C* and *D*, interaction between various Plk1 deletion mutants and endogenous p53. Whole cell lysates from COS7 cells transfected with the indicated expression plasmids were immunoprecipitated with monoclonal anti-FLAG antibody, and immunoblotted with monoclonal anti-p53 antibody to observe the interaction between Plk1 deletion mutants and p53. Immunoprecipitation with NMS was used as a negative control. Equal amounts of protein derived from cell lysates were immunoblotted with monoclonal anti-p53, monoclonal anti-FLAG, or polyclonal anti-actin antibody.

type p53 and these truncated forms of p53. As shown in Fig. 4C, wild-type p53 as well as p53 deletion mutants including p53-(1-359) and p53-(1-292), were detected in the anti-FLAG immunoprecipitates, whereas p53-(1-101) has lost the ability to bind to Plk1, indicating that the extreme COOH-terminal region, the oligomerization domain, and the NH₂-terminal transactivation domain of p53 are not involved in the interaction with Plk1. Similar immunoprecipitation analyses revealed that p53-(102-393) co-precipitates with FLAG-Plk1 (Fig. 4D). Thus, the region between amino acid residues 102 and 292 of p53, which includes the sequence-specific DNA-binding domain, appears to be required and sufficient for the interaction with Plk1.

Mapping of the p53-binding Region of Plk1—To map the p53-interacting domain on Plk1, we have constructed the FLAG-tagged Plk1 deletion mutants including Plk1-(1-401), Plk1-(1-329), and Plk1-(1-98) (Fig. 5A), and examined their subcellular localization by indirect immunofluorescent staining. As shown in Fig. 5B, COS7 cells transfected with each of the expression plasmids for FLAG-tagged Plk1 deletion mutants exhibited intense staining of the nucleus. Inspection of the amino acid sequence of Plk1-(1-98) identified one cluster of basic amino acids (⁴⁸RSRRRYVRGR⁵⁷), suggesting that this basic cluster acts as a nuclear localization signal. We then tested the interaction between p53 and each of these Plk1 deletion mutants. COS7 cells were transfected with the expres-

sion plasmid encoding Plk1-(1-401), Plk1-(1-329), or Plk1-(1-98), and co-immunoprecipitation experiments were performed to determine the interaction. We found that Plk1-(1-401) and Plk1-(1-329) retained the ability to bind to p53, whereas Plk1-(1-98) did not (Fig. 5C). These results indicate that the amino acid sequence comprising residues 99 to 329 of Plk1 contains the p53-binding domain.

Plk1 Inhibits the p53-mediated Transcriptional Activation—To determine whether Plk1 could affect the transcriptional activity of p53, H1299 cells were transiently co-transfected with a constant amount of the expression plasmid encoding p53 together with the p53-responsive *p21^{WAF1}*, *MDM2*, or *BAX*-luciferase reporter constructs in the presence or absence of increasing amounts of the expression plasmid for FLAG-Plk1. Under our experimental conditions, ectopically expressed p53 successfully activated the transcription of each of those p53-responsive reporters as compared with the empty plasmid controls, but Plk1 alone had no effect on luciferase activity (Fig. 6). Expression of FLAG-Plk1 greatly reduced the ability of p53 to increase the *p21^{WAF1}*, *MDM2*, and *BAX*-luciferase activities in a dose-dependent manner (Fig. 6, A-C). In addition, Plk1-(1-98), which lacks an ability to interact with p53, did not affect the p53 transcriptional activity toward the *p21^{WAF1}*, *MDM2*, and *BAX* promoters (data not shown). To confirm the inhibitory role of Plk1 in the p53-mediated transactivation, we assayed H1299 cell transfectants for induction of the endoge-

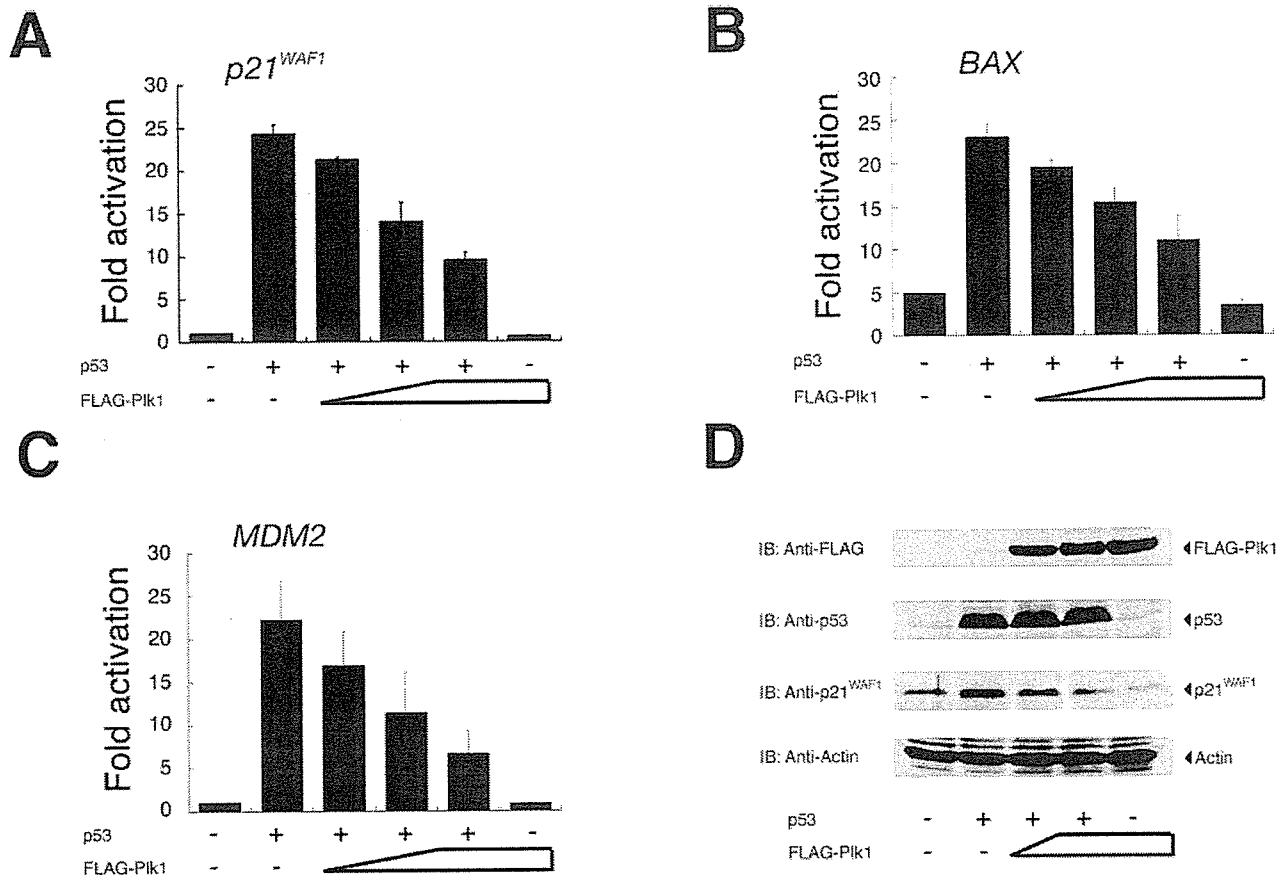


FIG. 6. Plk1 abrogates the p53-mediated transcriptional activation. p53-deficient H1299 cells (5×10^4 cells/well) were transiently co-transfected with 25 ng of the expression plasmid for p53 together with 100 ng of the luciferase reporter construct that carries the p53-responsive element derived from p21^{WAF1} (A), BAX (B), or MDM2 (C) promoter and 10 ng of the *Renilla* luciferase plasmid (pRL-TK) in the presence or absence of increasing amounts of pcDNA3-FLAG-Plk1 (50, 100, or 200 ng). The total amount of plasmid DNA per transfection was kept constant (510 ng) with pcDNA3. All transfections were performed in triplicate. Forty-eight hours after transfection, cells were lysed, and analyzed for their luciferase activities. Firefly luminescence signal was normalized based on the *Renilla* luminescence signal. Results are shown as -fold induction of the firefly luciferase activity compared with control cells transfected with pcDNA3 alone. D, immunoblot analysis. H1299 cells were transiently co-transfected with the indicated combinations of expression plasmids. Whole cell lysates were prepared 48 h post-transfection, and analyzed for the expression of FLAG-Plk1 (1st panel), p53 (2nd panel), or p21^{WAF1} (3rd panel) by immunoblot analysis with monoclonal anti-FLAG, monoclonal anti-p53, or polyclonal anti-p21^{WAF1} antibody, respectively. Total protein levels were controlled with polyclonal anti-actin antibody (4th panel).

nous p21^{WAF1}. To this end, H1299 cells were transiently co-transfected with a constant amount of the expression plasmid for p53 together with or without increasing amounts of the FLAG-Plk1 expression plasmid. Forty-eight hours after transfection, whole cell lysates were prepared and subjected to immunoblot analysis. Equal protein loading was confirmed by immunoblotting with the antibody against actin. As described (46), overexpression of p53 in H1299 cells resulted in the induction of the endogenous p21^{WAF1} compared with basal levels seen with empty plasmid (Fig. 6D, first and second lanes). Co-expression of p53 with FLAG-Plk1 caused a significant decrease in the endogenous p21^{WAF1} level in a dose-dependent manner (Fig. 6D, third and fourth lanes). These findings strongly suggest that Plk1 has an ability to inhibit p53-mediated transcriptional activation through physical interaction with p53.

To assess the possible effect of the endogenous Plk1 on the transcriptional activity of p53, we have employed an antisense strategy. As shown in Fig. 7A, expression of antisense *Plk1* in H1299 cells resulted in a reduction of the endogenous Plk1 as detected by immunoblot analysis. We then performed luciferase reporter analysis utilizing H1299 cells. As expected, co-expression of p53 with the antisense *Plk1* led to a slight but

significant increase in the p53-mediated transcriptional activation as compared with cells expressing p53 alone (Fig. 7, B-D).

Plk1 Inhibits the p53-mediated Apoptosis—To extend the functional significance of the physical interaction between Plk1 and p53, we next determined whether Plk1 could affect p53-mediated apoptosis. H1299 cells were transiently co-transfected with the expression plasmid encoding p53 together with or without the expression plasmid for FLAG-Plk1. Forty-eight hours after transfection, cell viability was monitored by a cell survival assay. As shown in Fig. 8A, overexpression of p53 resulted in a reduction of the number of viable cells as compared with that found in the control transfection, and Plk1 alone had little effect on cell viability. The reduced number of viable cells caused by exogenous p53 was recovered by co-expression of FLAG-Plk1. Considering that p53 induced apoptosis in transfected H1299 cells (47), Plk1 might abrogate the pro-apoptotic function of p53. To confirm this possibility, H1299 cells were transiently co-transfected with a constant amount of the GFP expression plasmid together with the indicated combinations of the expression plasmids. Forty-eight hours after transfection, transfected cells were scored by fluorescence microscopy for the appearance of green fluorescence,

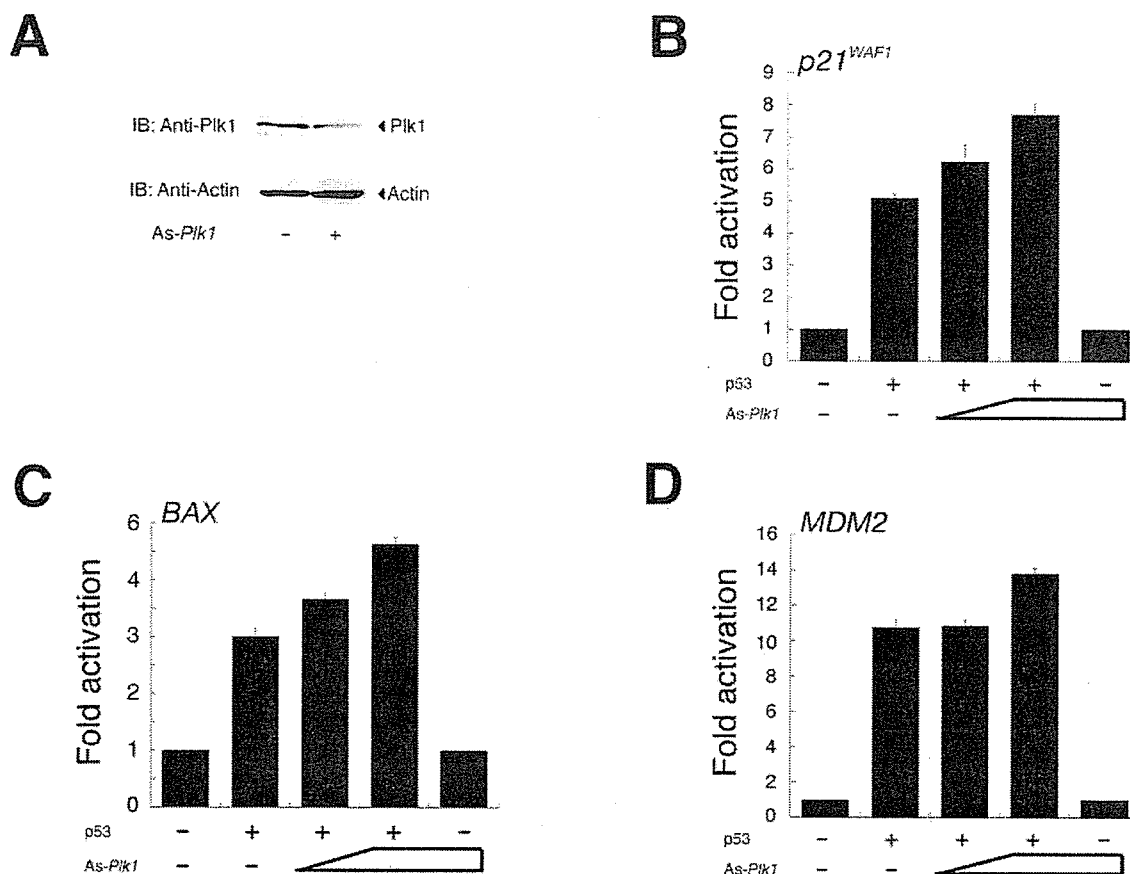


FIG. 7. Antisense *Plk1* increases the transcriptional activity of p53. *A*, antisense *Plk1* expression in H1299 cells results in a reduction of endogenous Plk1. H1299 cells were transfected with 2 μ g of antisense *Plk1* expression plasmid (*As-Plk1*). Whole cell lysates prepared from transfected cells were subjected to immunoblotting with the anti-Plk1 antibody (*top panel*). Western blotting for actin is shown as a control for protein loading (*bottom panel*). *B–D*, luciferase reporter analysis. H1299 cells were transiently co-transfected with 12.5 ng of the p53 expression plasmid along with 100 ng of the indicated luciferase reporter construct in the presence or absence of increasing amounts of *As-Plk1* (200 and 400 ng). Determination and calculation of the luciferase activities are described in the legend to Fig. 6.

and the number of GFP-positive cells with condensed and fragmented nuclei were counted. Under our experimental conditions, enforced expression of p53 led to an increase in the number of apoptotic cells as compared with the control transfection (Fig. 8B). In agreement with the above cell survival assay, co-expression of p53 with FLAG-Plk1 decreased the number of apoptotic cells as compared with that resulting from expression of p53 alone. Taken together, these results indicate that Plk1 is an efficient inhibitor of p53.

Kinase-deficient *Plk1* Fails to Inhibit p53—Next, we tested whether the Plk1 kinase activity could be required for Plk1-dependent inhibition of the p53 transcriptional activity. As described previously (22), the mutant form of Plk1 (Plk1-K82M), in which Lys⁸² within the ATP-binding motif is replaced by Met, completely lost the kinase activity. We therefore generated an expression plasmid encoding FLAG-Plk1(K82M), and then examined whether Plk1(K82M) could associate with p53, and also affect the p53-mediated transcriptional activation. Immunoprecipitation followed by Western detection of endogenous p53 indicated that p53 interacted with both the wild-type Plk1 and the kinase-deficient Plk1(K82M) (Fig. 9A). The effects of the lysine mutation on the p53-mediated transcriptional activation were tested by luciferase reporter analysis. In contrast to the wild-type Plk1, the kinase-deficient Plk1(K82M) failed to reduce the p53-mediated reporter expression driven by those constructs (Fig. 9, B–D).

To examine the effect of Plk1(K82M) on p53-dependent apoptosis, H1299 cells were transfected with the expression plas-

mid for p53 along with or without the expression plasmid for FLAG-Plk1(K82M). Forty-eight hours after transfection, their viability was measured by cell survival assay. As expected, the p53-dependent decrease in the number of viable cells was unaffected in the presence of the exogenous FLAG-Plk1(K82M) (Fig. 9E). Taken together, our results strongly suggest that the kinase activity of Plk1 is required for Plk1-dependent inhibition of p53.

ATM Antagonizes the Inhibitory Effect of Plk1 on p53—Plk1 kinase activity has been shown to be inhibited in an ATM-dependent manner in response to DNA damage (19, 20). The kinase activity of ATM was significantly increased after DNA damage, and ATM was able to phosphorylate p53 at the NH₂ terminus on serine 15 to enhance its stability as well as its transactivation activity (48–50). To examine whether ATM could affect the Plk1-mediated inhibition of p53, we transiently co-transfected H1299 cells with expression plasmids for p53 and FLAG-Plk1 together with or without increasing amounts of ATM expression plasmid, and the ability of p53 to drive transcription from the p21^{WAF1} reporter was measured. As expected, co-expression of p53 with ATM resulted in an increase in the transcriptional activity of p53 as compared with that of cells expressing p53 alone (Fig. 10). Increasing amounts of ATM largely abrogated the Plk1-mediated inhibition of the p53-dependent transcriptional activation. It thus appears that ATM could inhibit the activity of Plk1 and thereby restore the transcriptional activity of p53.

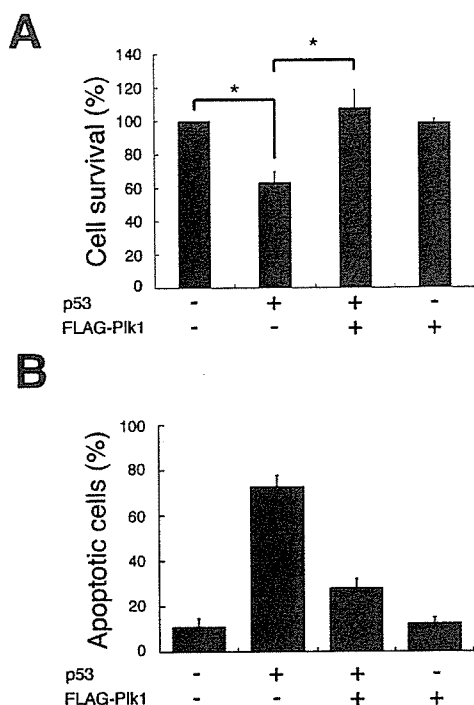


FIG. 8. Plk1 inhibits the pro-apoptotic activity of p53. **A**, H1299 cells were transiently co-transfected with 0.6 μg of the expression plasmid for p53 together with or without 1.2 μg of the FLAG-Plk1 expression plasmid. The total amount of plasmid DNA was kept constant (2 μg) with the empty plasmid. At 48 h after transfection, cell viability was determined by MTT cell survival assays. The graph (mean \pm S.D. of three independent experiments) represents relative viability based on the percent of viable cells compared with the control transfection (pcDNA3). The percentage of viable cells expressing p53 alone is significantly different from that of viable cells expressing p53 and FLAG-Plk1 ($p < 0.0001$). **B**, H1299 cells were transiently co-transfected with the indicated combinations of the expression plasmids. A constant amount of the GFP expression plasmid (200 ng) was included in all combinations, and the total amount of plasmid DNA was kept constant (2 μg) by including an appropriate amount of empty plasmid. Forty-eight hours after transfection, transfected cells were identified by the presence of green fluorescence. Cell nucleus was stained with propidium iodide to reveal nuclear condensation and fragmentation. The number of GFP-positive cells with condensed and fragmented nuclei was scored, and the percentage of apoptotic cells shown in each column represents the mean of three independent experiments.

DISCUSSION

In the present study, we have found that Plk1 interacts with p53 and inhibits its transactivation as well as apoptosis-inducing activity in mammalian cultured cells. This interaction is mediated by the sequence-specific DNA-binding domain of p53 and the region of Plk1 containing the kinase domain. Importantly, Plk1-mediated inhibition of p53 requires its kinase activity and is attenuated with ATM. Thus, our present data support the hypothesis that p53 is one of the critical targets of Plk1, and that Plk1-mediated inhibition of p53 contributes at least in part to cell fate decisions regarding survival and tumorigenesis.

The expression of *Plk1* was significantly down-regulated in response to cisplatin treatment. Recently, Ree *et al.* (51) found that ionizing radiation leads to the suppression of *Plk1* mRNA expression. It is of interest to examine whether genotoxic stresses other than cisplatin and ionizing radiation could also repress the expression of *Plk1*. On the other hand, *Plk1* mRNA expression is significantly induced in various human primary tumors (27). It is necessary to identify the promoter region as well as the transcription factor(s) required for the transcriptional regulation of *Plk1* in cancerous cells. In good agreement

with the previous observations (52), Uchiumi *et al.* (53) have identified the regulatory regions responsible for the activation of the human *Plk1* promoter, which include a consensus Sp1-binding site and a CCAAT box. It has been shown that the transcription factor NF-Y, a heterotrimeric complex consisting of NF-YA, NF-YB, and NF-YC, recognizes and binds to the CCAAT box (54). Indeed, the electrophoretic mobility shift assay revealed that NF-Y binds to the CCAAT box present within the human *Plk1* promoter region, however, it remains to be determined whether NF-Y and/or Sp1 could actually transactivate the *Plk1* promoter in tumor cells (53). Recently, Lee and Pedersen (55) have reported that there exist 6 GC boxes and the CCAAT box within the *type II hexokinase (HKII)* promoter, and that NF-Y and Sp family members including Sp1 might contribute to up-regulation of the *HKII* gene in tumor cells. Further studies regarding the transcriptional regulation of the *Plk1* gene are necessary to clarify the molecular mechanisms of Plk1-dependent tumorigenesis.

During the DNA damage response, the activity of ATM is significantly increased and is responsible for the rapid phosphorylation of p53 at Ser¹⁵ (48–50). This ATM-dependent phosphorylation contributes to the increased stability and activity of p53 by facilitating its dissociation from MDM2 (56). In addition, phosphorylation of p53 at Ser¹⁵ induces its binding to the transcriptional co-activator p300 (57). Recently, it has been shown that Plk1 activity is inhibited in response to DNA damage, and this inhibition occurs in an ATM-dependent manner (19, 20). Our present data demonstrate that the Plk1-mediated inhibition of p53 activity is rescued by the co-expression of ATM, suggesting that, in addition to the ATM-dependent phosphorylation of p53, the activity of p53 may be enhanced at least in part by the ATM-dependent inhibition of Plk1. Intriguingly, Liu and Erikson (33) reported that p53 is significantly stabilized in Plk1-depleted cells. In accordance with their findings, we have shown that the exposure of SH-SY5Y cells to cisplatin leads to a remarkable accumulation of p53, which is strongly associated with a significant down-regulation of the endogenous Plk1 both at mRNA and protein levels, suggesting that Plk1 is closely involved in the regulation of p53 stability and thereby modulates its activity. Under our experimental conditions, however, overexpression of FLAG-Plk1 did not affect the amounts of the endogenous as well as the ectopically expressed p53.

The pro-apoptotic function of p53 involves its ability to act as a transcription factor in transactivating downstream target gene promoters. The majority of missense mutations of p53 detected in human tumors occur within its sequence-specific DNA-binding domain, and these mutations cause the loss of p53 activity (58). Thus, the structural integrity of this domain is required for p53 function. On the other hand, several viral and cellular proteins inactivate p53 through a variety of different mechanisms (58). MDM2 and Pirh2 promote ubiquitination and degradation of p53 (59–62). Sir2 α interacts with p53 and induces its deacetylation (63). In addition, S100B calcium-binding protein prevents the oligomerization of p53 to inhibit its function (64). Based on our systematic immunoprecipitation analysis, Plk1 binds to p53 through the sequence-specific DNA-binding domain of p53. Intriguingly, SV40 large T antigen binds to the sequence-specific DNA-binding domain of p53, and abrogates DNA binding as well as the transactivation function of p53 (65, 66). It is thus likely that, like SV40 large T antigen, Plk1 might mask this domain of p53 by direct binding, and thereby inhibit its sequence-specific transcriptional activity. Further study is required to identify the detailed molecular mechanism.

In sharp contrast to Plk1, Xie *et al.* (26) found that the kinase

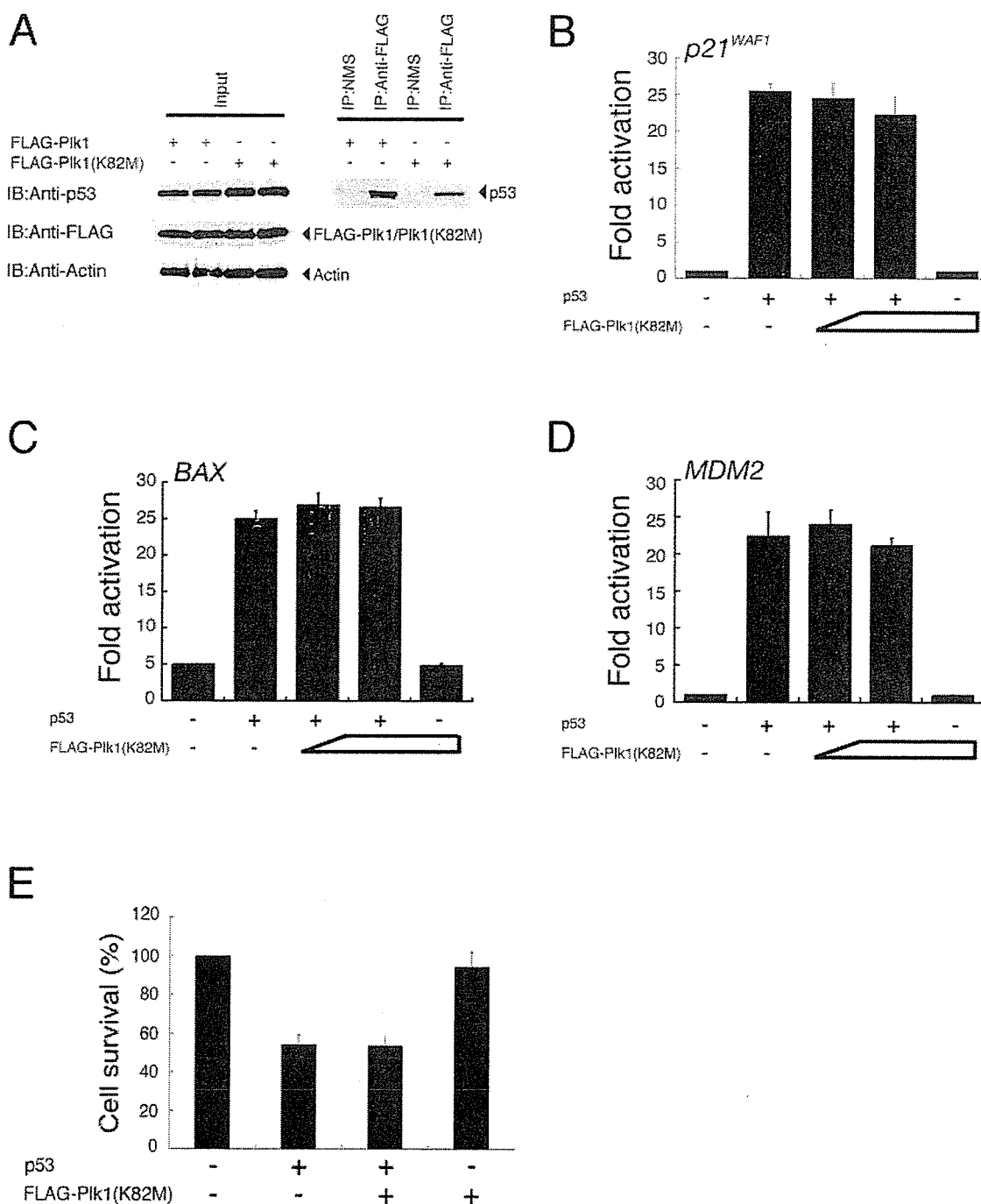


FIG. 9. Kinase-deficient Plk1(K82M) fails to reduce the activity of p53. *A*, Plk1(K82M) retains an ability to interact with p53. COS7 cells were transiently transfected with the expression plasmid for FLAG-Plk1 or FLAG-Plk1(K82M). Forty-eight hours after transfection, cell lysates were prepared and subjected to anti-FLAG immunoprecipitation followed by immunoblotting with monoclonal anti-p53 antibody. Immunoprecipitation with NMS was used as a negative control. Equal amounts of protein derived from cell lysates were immunoblotted with monoclonal anti-p53, monoclonal anti-FLAG, or with polyclonal anti-actin antibody. *B–D*, Plk1(K82M) has an undetectable effect on the transcriptional activity of p53. H1299 cells were transiently co-transfected with a fixed amount of the p53 expression plasmid (25 ng) and the p53-responsive luciferase reporter construct carrying the *p21^{WAF1}* (*B*), *BAX* (*C*), or *MDM2* (*D*) promoter (100 ng) in the presence or absence of increasing amounts of the expression plasmid encoding FLAG-Plk1(K82M) (100 or 200 ng). The total amount of plasmid DNA per transfection was kept constant (510 ng) with pcDNA3. Determination and calculation of the luciferase activities are described in the legend to Fig. 6. *E*, Plk1(K82M) is unable to inhibit the pro-apoptotic function of p53. H1299 cells were transiently co-transfected with the p53 expression plasmid (0.6 μ g) together with or without the expression plasmid for FLAG-Plk1(K82M) (1.2 μ g). Forty-eight hours after transfection, their viability was measured by MTT cell survival assays as described in the legend to Fig. 8.

activity of Plk3 is rapidly enhanced in response to DNA damage in an ATM-dependent fashion. They also described that Plk3 has the ability to interact directly with p53 and phosphorylate p53 at Ser²⁰. Moreover, a kinase-defective mutant form of Plk3

fails to phosphorylate p53, and abrogates the p53-mediated transcriptional activation as well as growth suppression, indicating that Plk3 might enhance the p53 activity through Ser²⁰ phosphorylation of p53 (26). In addition to Ser¹⁵ phosphoryla-

FIG. 10. ATM antagonizes the inhibitory effect of Plk1 on the p53-dependent transactivation. H1299 cells were transiently co-transfected with the expression plasmids encoding p53 (25 ng) and FLAG-Plk1 (200 ng) along with the luciferase reporter construct containing the p53-responsive element from the *p21^{WAF1}* promoter in the presence or absence of increasing amounts of ATM expression plasmid (50 or 100 ng). pcDNA3 was used to equalize the amount of plasmid in each transfection, and the *Renilla* luciferase plasmid was included in the transfection mixture to normalize the transfection efficiency. Determination and calculation of the luciferase activities are described in the legend to Fig. 6.

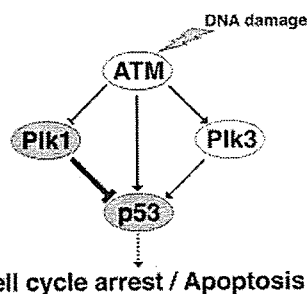
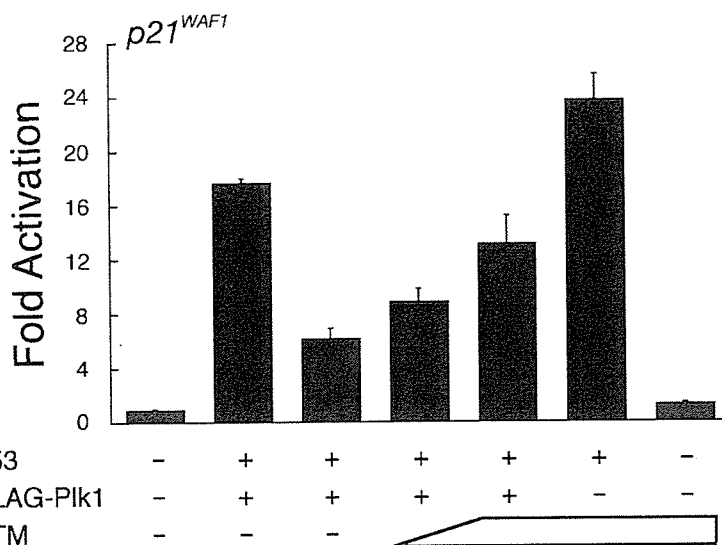


FIG. 11. Schematic representation of interactions among ATM, Plk1, Plk3, and p53 in response to DNA damage.

tion of p53, DNA damage-induced phosphorylation of p53 at Ser²⁰ prevents its association with MDM2 and results in its stabilization (67). Of note, it has been shown that Plk1 phosphorylates p53 *in vitro* but on residues that might be different from that mediated by Plk3 (26). According to their phosphopeptide mapping analysis, at least three unique radiolabeled tryptic peptides derived from recombinant p53 were detected in the presence of Plk1. Recently, Nakajima *et al.* (68) identified a sequence (D/E)X(S/T) ψ X(D/E) (X, any amino acid; ψ , a hydrophobic amino acid) as a consensus motif for Plk1-dependent phosphorylation (68). During the search for a putative phosphorylation site(s) targeted by Plk1 within the amino acid sequence of p53, we found a related motif (²⁵⁴IITLED²⁵⁹) present within the sequence-specific DNA-binding domain of p53, suggesting that this motif could be one of the putative phosphorylation sites of p53 targeted by Plk1, although there is no direct evidence for this possibility. According to our present results, the kinase-deficient mutant form of Plk1 that retained an ability to associate with p53, failed to reduce the transcriptional as well as apoptosis-inducing activity of p53, suggesting that the kinase activity of Plk1 is critical for the Plk1-dependent inhibition of p53. Thus, identification of the major phosphorylation site(s) of p53 by Plk1 is required to establish the functional significance of the Plk1-mediated phosphorylation of p53. In contrast, Liu and Erikson (33) reported that, like wild-type mouse Plk1, co-expression of the kinase-defective (K82M) mouse Plk1 partially rescued the apoptotic phenotype induced by the depletion of Plk1, indicating that the kinase activity is not necessary for its anti-apoptotic activity. They also described that their kinase-defective mouse Plk1 has 15–20% of wild-type kinase activity, raising a possibility that the residual kinase

activity of their mouse Plk1(K82M) might be enough to inhibit the Plk1 depletion-induced apoptosis.

Fig. 11 shows a model that incorporates our present findings, and illustrates various interactions in response to DNA damage. Given the fact that the differential expression of Plk1 and Plk3 during the cisplatin-induced apoptosis, and their differential effects on p53, it is conceivable that the balance between intracellular expression levels of Plk1 with oncogenic potential and pro-apoptotic Plk3 is at least in part responsible for the determination of the cell fate via the physical and functional interaction with p53.

Acknowledgments—We are grateful to Dr. Y. Shiloh and the Japanese Study Group for Pediatric Liver Tumor for kindly providing the ATM expression plasmid and hepatoblastoma tissues, respectively. We thank Dr. S. Sakiyama and members of our laboratory for helpful discussions. We also thank Y. Nakamura and M. Kikawa for excellent technical assistance.

REFERENCES

- Glover, D. M., Hagan, I. M., and Tavares, A. A. (1998) *Genes Dev.* **12**, 3777–3787
- Clay, F. J., McEwen, S. J., Bertoncello, I., Wilks, A. F., and Dunn, A. R. (1993) *Proc. Natl. Acad. Sci. U. S. A.* **90**, 4832–4866
- Lee, K. S., Grenfell, T. Z., Yarn, F. R., and Erikson, R. L. (1998) *Proc. Natl. Acad. Sci. U. S. A.* **95**, 9301–9306
- Song, S., Grenfell, T., Garfield, S., Erikson, R. L., and Lee, K. S. (2000) *Mol. Cell Biol.* **20**, 286–298
- Jang, Y.-J., Lin, C.-Y., Ma, S., and Erikson, R. L. (2002) *Proc. Natl. Acad. Sci. U. S. A.* **99**, 1984–1989
- Glover, D. M., Ohkura, H., and Tavares, A. (1996) *J. Cell Biol.* **135**, 1631–1684
- Lane, H., and Nigg, E. A. (1997) *Trends Cell Biol.* **7**, 63–68
- Nigg, E. A. (1998) *Curr. Opin. Cell Biol.* **10**, 776–783
- Hamanaka, R., Maloid, S., Smith, M. R., O'Connell, C. D., Longo, D. L., and Ferris, D. K. (1994) *Cell Growth & Differ.* **5**, 249–257
- Smith, M. R., Wilson, M. L., Hamanaka, R., Chase, D., Kung, H.-F., Longo, D. L., and Ferris, D. K. (1997) *Biochem. Biophys. Res. Commun.* **234**, 397–405
- Lake, R. J., and Jelinek, W. R. (1993) *Mol. Cell Biol.* **13**, 7793–7801
- Golsteyn, R. M., Schultz, S. J., Bartek, J., Ziemiński, A., Ried, T., and Nigg, E. A. (1994) *J. Cell Sci.* **107**, 1509–1517
- Holtrich, U., Wolf, G., Brauning, A., Karn, T., Bohme, E., Rubsamen-Waigmann, H., and Strebhardt, K. (1994) *Proc. Natl. Acad. Sci. U. S. A.* **91**, 1736–1740
- Simmons, D. L., Neel, B. G., Stevens, R., Evett, G., and Erikson, R. L. (1992) *Mol. Cell Biol.* **12**, 4164–4169
- Donohue, P. J., Alberts, G. F., Guo, Y., and Winkles, J. A. (1995) *J. Biol. Chem.* **270**, 10351–10357
- Golsteyn, R. M., Mundt, K. E., Fry, A. M., and Nigg, E. A. (1995) *J. Cell Biol.* **129**, 1617–1628
- Hamanaka, R., Smith, M. R., O'Connor, P. M., Maloid, S., Mihalic, K., Spivak, J. L., Longo, D. L., and Ferris, D. K. (1995) *J. Biol. Chem.* **270**, 21086–21091
- Qian, Y.-W., Erikson, E., and Maller, J. L. (1993) *Science* **262**, 1701–1704
- Smits, V. A., Klompaker, R., Arnaud, L., Rijkssen, G., Nigg, E. A., and Medema, R. H. (2000) *Nat. Cell Biol.* **2**, 672–676
- van Vugt, M. A. T. M., Smits, V. A. J., Klompaker, R., and Medema, R. H. (2001) *J. Biol. Chem.* **276**, 41656–41660
- Toyoshima-Morimoto, F., Taniguchi, E., Shinya, N., Iwamatsu, A., and

- Nishida, E. (2001) *Nature* **410**, 215–220
22. Yuan, J., Eckerdt, F., Bereiter-Hahn, J., Kurunci-Csacsko, E., Kaufmann, M., and Strebhardt, K. (2002) *Oncogene* **21**, 8282–8292
 23. Toyoshima-Morimoto, F., Taniguchi, E., and Nishida, E. (2002) *EMBO Rep.* **3**, 341–348
 24. Ouyang, B., Pan, H., Lu, L., Li, J., Stambrook, P., Li, B., and Dai, W. (1997) *J. Biol. Chem.* **272**, 28646–28651
 25. Bahassi, E. M., Conn, C. W., Myer, D. L., Hennigan, R. F., McGowan, C. H., Sanchez, Y., and Stambrook, P. J. (2002) *Oncogene* **21**, 6633–6640
 26. Xie, S., Wu, H., Wang, Q., Cogswell, J. P., Husain, I., Conn, C., Stambrook, P., Jhanwar-Uniyal, M., and Dai, W. (2001) *J. Biol. Chem.* **276**, 43305–43312
 27. Yuan, J., Horlin, A., Hock, B., Stutte, H. J., Rubsamen-Waigmann, H., and Strebhardt, K. (1997) *Am. J. Pathol.* **150**, 1165–1172
 28. Wolf, G., Elez, R., Doermer, A., Holtrich, U., Ackermann, H., Stutte, H. J., Altmannsberger, H. M., Rubsamen-Waigmann, H., and Strebhardt, K. (1997) *Oncogene* **14**, 543–549
 29. Knecht, R., Elez, R., Oechler, M., Solbach, C., von Ilberg, C., and Strebhardt, K. (1999) *Cancer Res.* **59**, 2794–2797
 30. Knecht, R., Oberhauser, C., and Strebhardt, K. (2000) *Int. J. Cancer* **89**, 535–536
 31. Spankuch-Schmitt, B., Wolf, G., Solbach, C., Loibl, S., Knecht, R., Stegmüller, M., von Minckwitz, G., Kaufmann, M., and Strebhardt, K. (2002) *Oncogene* **21**, 3162–3171
 32. Spankuch-Schmitt, B., Bereiter-Hahn, J., Kaufmann, M., and Strebhardt, K. (2002) *J. Natl. Cancer Inst.* **94**, 1863–1877
 33. Liu, X., and Erikson, R. L. (2003) *Proc. Natl. Acad. Sci. U.S.A.* **100**, 5789–5794
 34. Li, B., Ouyang, B., Pan, H., Reissmann, P. T., Slamon, D. J., Arceci, R., Lu, L., and Dai, W. (1996) *J. Biol. Chem.* **271**, 19402–19408
 35. Dai, W., Li, Y., Ouyang, B., Pan, H., Reissmann, P., Li, J., Wiest, J., Stambrook, P., Gluckman, J. L., Noffsinger, A., and Bejarano, P. (2000) *Genes Chromosomes Cancer* **27**, 332–336
 36. Conn, C. W., Hennigan, R. F., Dai, W., Sanchez, Y., and Stambrook, P. J. (2000) *Cancer Res.* **60**, 6826–6831
 37. Xie, S., Wang, Q., Wu, H., Cogswell, J., Lu, L., Jhanwar-Uniyal, M., and Dai, W. (2001) *J. Biol. Chem.* **276**, 36194–36199
 38. Nakamura, Y., Ozaki, T., Nakagawara, A., and Sakiyama, S. (1997) *Eur. J. Cancer* **33**, 1986–1990
 39. Nakagawa, T., Takahashi, M., Ozaki, T., Watanabe, K., Todo, S., Mizuguchi, H., Hayakawa, T., and Nakagawara, A. (2002) *Mol. Cell. Biol.* **22**, 2575–2585
 40. Watanabe, K., Ozaki, T., Nakagawa, T., Miyazaki, K., Takahashi, M., Hosoda, M., Hayashi, S., Todo, S., and Nakagawara, A. (2002) *J. Biol. Chem.* **277**, 15113–15123
 41. Kim, E.-J., Park, J.-S., and Um, S.-J. (2002) *J. Biol. Chem.* **277**, 32020–32028
 42. Taniguchi, E., Toyoshima-Morimoto, F., and Nishida, E. (2002) *J. Biol. Chem.* **277**, 48884–48888
 43. Kastan, M. B., Zhan, Q., el-Deiry, W. S., Carrier, F., Jacks, T., Walsh, W. V., Plunkett, B. S., Vogelstein, B., and Fornace, A. J., Jr. (1992) *Cell* **71**, 587–597
 44. Shaulsky, G., Goldfinger, N., Ben-Ze'ev, A., and Rotter, V. (1990) *Mol. Cell. Biol.* **10**, 6565–6577
 45. Dang, C. V., and Lee, W. M. (1989) *J. Biol. Chem.* **264**, 18019–18023
 46. Zaika, A. L., Slade, N., Erster, S. H., Sansome, C., Joseph, T. W., Pearl, M., Chalas, E., and Moll, U. M. (2002) *J. Exp. Med.* **196**, 765–780
 47. Zeng, X., Chen, L., Jost, C. A., Maya, R., Keller, D., Wang, X., Kaelin, W. G., Oren, M., Chen, J., and Lu, H. (1999) *Mol. Cell. Biol.* **19**, 3257–3266
 48. Banin, S., Moyal, L., Shieh, S., Taya, Y., Anderson, C. W., Chessa, L., Smorodinsky, N. I., Prives, C., Reiss, Y., Shiloh, Y., and Ziv, Y. (1998) *Science* **281**, 1674–1677
 49. Canman, C. E., Lim, D. S., Cimprich, K. A., Taya, Y., Tamai, K., Sakaguchi, K., Appella, E., Kastan, M. B., and Siliciano, J. D. (1998) *Science* **281**, 1677–1679
 50. Khanna, K. K., Keating, K. E., Kozlov, S., Scott, S., Gatei, M., Hobson, K., Taya, Y., Gabrielli, B., Chan, D., Lees Miller, S. P., and Lavin, M. F. (1998) *Nat. Genet.* **20**, 398–400
 51. Ree, A. H., Bratland, A., Nome, R. V., Stokke, T., and Fodstad, O. (2003) *Oncogene* **22**, 8952–8955
 52. Brauninger, A., Strebhardt, K., and Rubsamen-Waigmann, H. (1995) *Oncogene* **11**, 1793–1800
 53. Uchiyama, T., Longo, D. L., and Ferris, D. K. (1997) *J. Biol. Chem.* **272**, 9166–9174
 54. Mantovani, R. (1999) *Gene (Amst.)* **239**, 15–27
 55. Lee, M. G., and Pedersen, P. L. (2003) *J. Biol. Chem.* **278**, 41047–41058
 56. Shieh, S. Y., Ikeda, M., Taya, Y., and Prives, C. (1997) *Cell* **91**, 325–334
 57. Lambert, P. F., Kashanchi, F., Radonovich, M. F., Shiekhhattar, R., and Brady, J. N. (1998) *J. Biol. Chem.* **273**, 33048–33053
 58. Prives, C., and Hall, P. A. (1999) *J. Pathol.* **187**, 112–126
 59. Haupt, Y., Maya, R., Kazaz, A., and Oren, M. (1997) *Nature* **387**, 296–299
 60. Kubbutat, M. H. G., Jones, S. N., and Vousden, K. H. (1997) *Nature* **387**, 299–303
 61. Honda, R., Tanaka, H., and Yasuda, Y. (1997) *FEBS Lett.* **420**, 25–27
 62. Leng, R. P., Lin, Y., Ma, W., Wu, H., Lemmers, B., Chung, S., Parant, J. M., Lozano, G., Hakem, R., and Benchimol, S. (2003) *Cell* **112**, 779–791
 63. Luo, J., Nikolaev, A. Y., Imai, S., Chen, D., Su, F., Shiloh, A., Guarente, L., and Gu, W. (2001) *Cell* **107**, 137–148
 64. Lin, J., Blake, M., Tang, C., Zimmer, D., Rustandi, R. R., Weber, D. J., and Carrier, F. (2001) *J. Biol. Chem.* **276**, 35037–35041
 65. Tan, T.-H., Wallis, J., and Levine, A. J. (1986) *J. Virol.* **59**, 574–583
 66. Farmer, G., Bargonetti, J., Zhu, H., Friedman, P., Prywes, R., and Prives, C. (1992) *Nature* **358**, 83–86
 67. Vousden, K. H. (2002) *Biochim. Biophys. Acta* **1602**, 47–59
 68. Nakajima, H., Toyoshima-Morimoto, F., Taniguchi, E., and Nishida, E. (2003) *J. Biol. Chem.* **278**, 25277–25280

Reduced inflammatory pain in mice deficient in the differential screening-selected gene aberrative in neuroblastoma

S. Ohtori,^{a,1} E. Isogai,^{b,1} F. Hasue,^a T. Ozaki,^b Y. Nakamura,^b A. Nakagawara,^b H. Koseki,^c S. Yuasa,^d E. Hanaoka,^a J. Shinbo,^a T. Yamamoto,^e H. Chiba,^f M. Yamazaki,^a H. Moriya,^a and S. Sakiyama^{b,*}

^aDepartment of Orthopaedic Surgery, Graduate School of Medicine, Chiba University, Chuo, Chiba 260-8677, Japan

^bDivision of Biochemistry, Chiba Cancer Center Research Institute, Chuo, Chiba 260-8717, Japan

^cDepartment of Molecular Embryology, Graduate School of Medicine, Chiba University, Chuo, Chiba 260-8677, Japan

^dNational Institute of Neuroscience, Kodaira, Tokyo 187-8502, Japan

^eDepartment of Anaesthesiology, Graduate School of Medicine, Chiba University, Chuo, Chiba 260-8677, Japan

^fThird Department of Anatomy, Graduate School of Medicine, Chiba University, Chuo, Chiba 260-8677, Japan

Received 10 February 2003; revised 21 November 2003; accepted 1 December 2003

Differential screening-selected gene aberrative in neuroblastoma (*Dan*) protein is produced in small neurons of dorsal root ganglia. Thermal and mechanical allodynia and Fos expression in the spinal dorsal horn evoked by inflammation and neuropathic pain were investigated using *Dan*-deficient mice. Mice showed pain reactions induced by the introduction of complete Freund's adjuvant (CFA) into their hind paw (inflammatory pain model) and after sciatic nerve ligation (neuropathic pain model). In the inflammatory pain model, thermal and mechanical pain thresholds in *Dan*-deficient mice were significantly higher than those of wild-type mice. The number of Fos-immunoreactive cells in the dorsal horn during the inflammatory period was significantly less in *Dan*-deficient mice. However, in the neuropathic pain model, no differences in thermal hypersensitivity, mechanical allodynia, or the number of Fos-immunoreactive cells in the dorsal horn were observed between the mice. These data suggest that *Dan* may be a neuromodulator in inflammatory pain.

© 2004 Elsevier Inc. All rights reserved.

Introduction

The differential screening-selected gene aberrative in neuroblastoma (*Dan*) was initially cloned as an mRNA down-regulated in *v-src*-transformed rat fibroblasts (Ozaki and Sakiyama, 1993). The analysis of *Dan* function by transfection of cultured cells revealed that *Dan* has an ability to suppress the transformed phenotype and delay entry into the S phase, suggesting that *Dan* carries a tumor-suppressive activity (Ozaki and Sakiyama, 1994; Ozaki et al., 1995). Recently, it has been shown that *Dan* is a founding member of a novel gene family that includes the *Xenopus* head-inducing factor,

Cerberus and the dorsalizing factor, *Gremlin* (Hsu et al., 1998). *Dan* family members play crucial roles in early mouse embryonic development by inhibiting the signaling derived from bone morphogenetic proteins (BMPs) as well as modulating the action of transforming growth factor β (TGF- β) superfamily members (Hsu et al., 1998; Pearce et al., 1999; Piccolo et al., 1999; Stanley et al., 1998). Dionne et al. (2001) showed that *Dan*-deficient mice displayed subtle and background-dependent defects, suggesting that functional redundancy exists among *Dan* family members.

We previously showed the existence of *Dan* in primary small-diameter sensory nerve fibers, and also demonstrated that *Dan* mediates inflammatory pain, but not pain due to nerve injury (Ohtori et al., 2002). However, the precise mechanism underlying this action is unknown. In the present study, we have produced *Dan*-deficient mice and investigated inflammation and nerve injury-evoked thermal and mechanical allodynia and Fos expression in the spinal dorsal horn of *Dan*-deficient and wild-type mice.

Results and discussion

Generation of *Dan*-deficient mice

Mice with disrupted *Dan* alleles were generated using homologous recombination in embryonic stem cells to replace exons II and III with a neomycin-resistant gene (Fig. 1A). Genotyping of mutant mice was performed by Southern blot (Fig. 1B) and PCR (Fig. 1C) analyses using the probes and primers, respectively, as indicated in Fig. 1A. *Dan* mRNA was expressed in several organs in wild-type mice; however, as expected, it was not detected in *Dan*-deficient mice (Fig. 1D). Dionne et al. (2001) reported that *Dan*-deficient mice do not show apparent defects. In the current study, *Dan*-deficient mice did not show obvious differences when compared with wild-type mice during development, infancy, and adulthood. In the central and peripheral nervous systems, there were no morphologic changes in the *Dan*-deficient mice.

* Corresponding author. Division of Biochemistry, Chiba Cancer Center Research Institute, 666-2 Nitona, Chuo, Chiba 260-8717, Japan. Fax: +81-43-265-4459.

E-mail address: ssakiyam@chiba-cc.pref.chiba.jp (S. Sakiyama).

¹ These authors have contributed equally to this work.

Available online on ScienceDirect (www.sciencedirect.com.)